



# Development of Cortical Pyramidal Cell and Interneuronal Dendrites: a Role for Kainate Receptor Subunits and NETO1

Alexander Jack<sup>1</sup> · Mohammad I. K. Hamad<sup>1,2</sup> · Steffen Gonda<sup>1</sup> · Sebastian Gralla<sup>1</sup> · Steffen Pahl<sup>3</sup> · Michael Hollmann<sup>3</sup> · Petra Wahle<sup>1</sup>

Received: 25 June 2018 / Accepted: 25 October 2018 / Published online: 12 November 2018  
© Springer Science+Business Media, LLC, part of Springer Nature 2018

## Abstract

During neuronal development, AMPA receptors (AMPA) and NMDA receptors (NMDARs) are important for neuronal differentiation. Kainate receptors (KARs) are closely related to AMPARs and involved in the regulation of cortical network activity. However, their role for neurite growth and differentiation of cortical neurons is unclear. Here, we used KAR agonists and overexpression of selected KAR subunits and their auxiliary neuropilin and tolloid-like proteins, NETOs, to investigate their influence on dendritic growth and network activity in organotypic cultures of rat visual cortex. Kainate at 500 nM enhanced network activity and promoted development of dendrites in layer II/III pyramidal cells, but not interneurons. GluK2 overexpression promoted dendritic growth in pyramidal cells and interneurons. GluK2 transfectants were highly active and acted as drivers for network activity. GluK1 and NETO1 specifically promoted dendritic growth of interneurons. Our study provides new insights for the roles of KARs and NETOs in the morphological and physiological development of the visual cortex.

**Keywords** Rat neocortex · Postnatal development · Dendritogenesis · Glutamate receptors · GluK2 · NETO

## Introduction

In the mammalian CNS, L-glutamate is the principal excitatory neurotransmitter for fast synaptic transmission. It acts via AMPA (GluA), NMDA (GluN), and kainate receptors (GluK) [1, 2]. AMPARs, NMDARs, and KARs are essential for neuronal development and display distinct functions in regulating synaptic transmission and plasticity. For instance, in tadpole optic tectum neurons, the maturation of the complex dendritic trees has been

shown to be dependent on activity and calcium signaling triggered by NMDARs [3]. Blocking NMDARs impairs dendritic development evoked by visual synaptic activity [4, 5]. In the rodent barrel cortex, deletion of the GluN1 subunit leads to abnormal development of dendritic patterns [6, 7]. Disruption of GluA2 decreases dendritic complexity in the frog optic tectum [8]. In slice cultures of rat visual cortex, overexpression of distinct splice variants of AMPARs differentially regulates the morphological maturation of pyramidal cells and interneurons. Interestingly, the AMPAR flip isoforms with prolonged channel opening times are more efficient than flop isoforms and calcium-permeable AMPARs [9]. Moreover, type-I transmembrane AMPA receptor regulatory proteins (TARPs) enhance dendritic maturation of cortical pyramidal cells by augmented trafficking of endogenous AMPARs [10]. The growth response requires NMDARs and voltage-gated calcium channels (VGCCs). In a developmental context, the role of KARs and NETOs for dendritogenesis in the neocortex has remained elusive.

KARs are represented by three low-affinity subunits, GluK1, 2, 3, and two high-affinity subunits, GluK4, 5 [11]. KARs are expressed as homo- and heterotetramers of various subunit combinations; only GluK1-3 can form functional homomeric channels, whereas GluK4/5 co-assemble with low-affinity subunits [12]. KARs diversify by RNA editing

**Electronic supplementary material** The online version of this article (<https://doi.org/10.1007/s12035-018-1414-0>) contains supplementary material, which is available to authorized users.

✉ Petra Wahle  
petra.wahle@rub.de

<sup>1</sup> Faculty for Biology and Biotechnology ND 6/72, Developmental Neurobiology, Ruhr University Bochum, Universitätsstraße 150, 44801 Bochum, Germany

<sup>2</sup> Medical Faculty, Neuroanatomy and Molecular Brain Research, Ruhr University Bochum, Universitätsstraße 150, 44801 Bochum, Germany

<sup>3</sup> Faculty of Chemistry and Biochemistry, Biochemistry I—Receptor Biochemistry, Ruhr University Bochum, Universitätsstraße 150, 44801 Bochum, Germany

to control calcium permeability and by alternative splicing [13]. In rodent cortex, GluK2 and GluK5 are the most abundant subunits [14, 15] with pyramidal cells mainly expressing GluK2 [12, 16], while interneurons abundantly express GluK1 [17–19]. Pre- and postsynaptically located KARs modulate transmitter release and network excitability, respectively, through ionotropic and also metabotropic pathways [13, 20–22].

Compared to AMPARs and NMDARs, an involvement of KARs in neuronal maturation has not been tested as extensively. Monnerie and Le Roux 2006 [23] have shown that exposing E18 dissociated mouse cortical neurons for 3 days to 10–100  $\mu$ M kainate increases the number of primary dendrites and dendritic length in an NBQX- and NS-102-sensitive fashion. Kainate at low concentrations (300 nM) enhances neurite outgrowth of cultured mouse dorsal root ganglion neurons (DRGs) [24] and higher concentrations have been shown to stop neurite outgrowth in DRGs [25]. Kainate at low concentrations increases the amplitude of EPSCs in supragranular cortical pyramidal cells [26], and our study on AMPAR revealed that larger amplitudes are efficient inducers of dendritic growth [9]. However, KARs usually desensitize fast, and can become quickly internalized in a PKC-dependent fashion when activity increases [27, 28]. Yet, KARs may influence growth via metabotropic actions, for instance by enhanced recycling of AMPARs to synaptic membranes; this has recently been shown to contribute to hippocampal LTP [29]. Moreover, in neonatal hippocampus, activation of presumably presynaptic KARs by 50 nM kainate contributes to network activity [30], and perinatal network activity is discussed as a driver for morphological maturation [5]. NETO1 contributes to the development of hippocampal circuitry by regulating axonal and presynaptic KARs [31]. In DRGs, NETO2 plays a crucial and dynamic role in neurite outgrowth during development and in adult DRGs [32].

In the present study, we used KAR-targeting pharmaca as well as overexpression of selected KAR and NETO subunits to systematically investigate their role in dendritic growth during early postnatal development. The results suggest that GluK2 contributes to pyramidal cell dendritic maturation, cellular excitability, and network activity. Moreover, GluK1 as well as NETO1 enhance dendritic maturation of interneurons.

## Methods

### Organotypic Cultures

Visual cortex organotypic cultures (OTCs) were prepared from P0/1 newborn rat pups (Long Evans) as described [33]. Tissue was chopped in 350  $\mu$ m slices using a McIlwain tissue chopper (Ted Pella, Redding, CA, USA) and mounted on a coverslip with a plasma/thrombin clot. OTCs were kept at

37 °C in roller tubes supplied with 700  $\mu$ l semi-artificial medium containing 25% adult horse serum, 25% Hank's balanced salt solution, 50% Eagle's Basal Medium, 1 mM L-glutamine (all from Life Technologies, Karlsruhe, Germany), and 0.65% D-Glucose (Merck, Darmstadt, Germany). To prevent excessive glial growth, OTCs were treated at DIV 2 (DIV = days in vitro) with a cocktail of uridine, cytosine- $\beta$ -D-arabino-furanosid, and 5-fluorodeoxyuridine (all from Sigma-Aldrich, Steinheim, Germany) for 24 h. Medium was changed every third day for transfected OTCs which did not receive any pharmacological treatment. All data presented derived from minimum of two, mostly three independent culture preparations each done from four to five pups. Slices from every individual were allocated to all experimental conditions of the respective experiment. For calcium imaging, OTC medium was changed to artificial cerebrospinal fluid (ACSF) containing in mM: 125 NaCl, 5 KCl, 2 CaCl<sub>2</sub>, 1 MgSO<sub>4</sub>, 25 NaHCO<sub>3</sub>, 1.25 NaH<sub>2</sub>PO<sub>4</sub>, 25 glucose, pH 7.4.

### Expression Plasmids

All plasmids (see Supplementary Table 1) were prepared as endotoxin-free solutions using the EndoFree Plasmid Maxi Kit (Qiagen, Cat No./ID: 12362). Plasmid stocks were diluted to 1  $\mu$ g/ $\mu$ l and stored at –20 °C.

### Pharmacological Treatment

For pharmacological treatment to test the involvement of L-type voltage-gated calcium channels, NMDARs or AMPARs, OTCs were kept under nifedipine (10  $\mu$ M; Sigma-Aldrich, Steinheim, Germany), or DL-2-amino-5-phosphonovaleric acid (APV, 50  $\mu$ M; Sigma-Aldrich, Deisenhofen, Germany), or GYKI 47261 (1  $\mu$ M; Tocris, Wiesbaden, Germany) from DIV 5–10 concomitant with the overexpression of the GluK2(R) subunit. For chronic stimulation, OTCs were kept under final concentrations in the medium of 500 nM kainate, or 1  $\mu$ M ATPA, or 1  $\mu$ M UBP 310 (all from Tocris, Wiesbaden, Germany) from DIV 5–10. Medium was refreshed every second day in order avoid accumulation of pharmaca. To test the involvement of metabotropic actions on the kainate-induced increase in network activity, we divided two large batches of cultures into two groups: one for calphostin C and one for H89. From the two batches, 2  $\times$  5 OTC have been recorded. The PKC inhibitor calphostin C (1  $\mu$ M; Tocris, Wiesbaden, Germany) or the PKA inhibitor H89 (10  $\mu$ M; Tocris, Wiesbaden, Germany) were added to the recording chamber for 30 min after baseline activities were recorded and could be increased by 500 nM kainate. Afterwards, calphostin C or H89 were washed out with ACSF containing 500 nM kainate for 10 min before activity was subsequently recorded.

## Biolistic Transfection

Transfection was carried out as described [9, 10, 33]. Briefly, cartridges were prepared by coating 10 mg gold microcarriers (1  $\mu\text{m}$  diameter; BioRad) with 10  $\mu\text{g}$  plasmid encoding the reporter (EGFP or mCherry) alone or in combination with 10  $\mu\text{g}$  of the plasmid encoding one of the effector proteins (KAR subunits, NETOs, TTBK2-KD). TTBK2-KD was a gift from Dario Alessi [34]. For confocal calcium imaging, the calcium sensor GCaMP6m (pGP-CMV-GCaMP6m, a gift from Douglas Kim [35]) served as a reporter and was cotransfected with one of the effector proteins. Although GCaMP6m shows very low baseline fluorescence, cells could easily be selected for imaging when fluorescence increased upon activity. Cultures were blasted at DIV 5 using the hand-held Helios Gene Gun (BioRad, Munich, Germany) with 180 psi helium pressure. In order to test if the morphological development of wild-type neurons wired up in a network containing GluK2(R) transfectants is affected by the increased network activity, two blasts to OTCs were delivered: the first blast delivered EGFP and the second blast delivered mCherry; this is the control condition. For the experimental condition, the first blast delivered EGFP together with GluK2(R) and the second blast delivered mCherry. This way, we labeled two separate neuronal subsets in every culture. The probability that one cell is occasionally double-transfected by two blasts (mCherry-coated particle striking the same cell that was previously hit by GluK(R) + EGFP) is very low. Still, prior to fixation, every OTC was checked for transfectants positive for both EGFP and mCherry. This was indeed the case in a few OTCs and these OTCs were discarded. After 5 days of overexpression, the mCherry-labeled layer II/III pyramidal cells were reconstructed. We focused only on this population because they were the ones strongly responding to GluK2 overexpression.

## Immunohistochemistry and Immunofluorescence

For morphometrical analysis, OTCs were fixed with pre-warmed (37  $^{\circ}\text{C}$ ) 4% paraformaldehyde in 0.1 M phosphate buffer pH 7.4 at DIV 10 for 2 h. Immunohistochemistry against EGFP or mCherry was done as described [9, 33] using a mouse antibody against GFP (1:1000; clone GSN24, Sigma-Aldrich, RRID: AB\_563117) or mCherry (Living Colors®, Clontech, Hamburg, Germany, RRID AB\_2307319) overnight followed by biotinylated goat anti-mouse (1:1000; Dako A/S, Glostrup, Denmark, product no. E043301-2) for 3 h, ABC reagent for 2 h (Vector Laboratories Inc., Burlingame, CA, USA, Cat# PK-7100; RRID: AB\_2336827), and reacted with 3,3'-diaminobenzidine (Sigma-Aldrich, Steinheim, Germany) and  $\text{H}_2\text{O}_2$ . The DAB reaction product was intensified with  $\text{OsO}_4$  (Sigma-Aldrich, Steinheim, Germany). Subsequently, cultures were

dehydrated and coverslipped with DEPEX (Sigma-Aldrich, Steinheim, Germany). For fluorescent staining, OTCs were transfected with the fluorophore-tagged receptor subunits (GluK2(R)-pEGFP or GluA2(R)-i-pEYFP, respectively) at DIV 5. After 3 days of overexpression, OTCs were fixed and incubated with the GFP antibody as described above. Subsequently, incubation with fluorescent secondary antibodies (1:500 goat anti-mouse ALEXA-488, Thermo Fisher Scientific Cat# A-11001, RRID: AB\_2534069) was done for 1 h to enhance the signal. After incubation, OTCs were washed 3 $\times$  with TBS, 3 $\times$  with PBS, coverslipped with sRIMS [36], sealed with nail polish, and imaged.

## Morphometrical Analysis

Immunostained neurons were reconstructed with the NeuroLucida system (MicroBrightField, Inc., Williston, Vermont, USA) as described [10] by observers blinded to experimental conditions. Reconstructed cells were cross-checked and classified by a second observer, who was also blinded to condition. No preselection of cells was done. Pyramidal cells and interneurons were distinguished by criteria of dendritic and axonal patterns [9, 33].

## Kainate-Induced Dendritic Injury Assay

At DIV 10, OTCs overexpressing EGFP alone or together with the effector proteins indicated (KAR subunits, TTBK2-KD) were challenged with 25  $\mu\text{M}$  kainate for 10 min in the roller incubator, followed by fixation with pre-warmed 4% phosphate-buffered paraformaldehyde and immunostained against EGFP as described above. The percentage of transfected neurons with symptoms of dendritic beading was determined by two observers blinded to conditions as described [9, 10] (for representative neurons displaying dendritic beading, see Supplementary Fig. 1A).

## Two-Photon and Confocal Calcium Imaging

OTCs were allowed to express EGFP alone or together with effector proteins for a minimum of 2 days before recording. On the day of recording, cultures were loaded with Oregon Green® 488 BAPTA-1 AM (OGB; Molecular Probes, Oregon, USA) as described [37] and subsequently washed with oxygenated ACSF. After loading, OGB was washed out with oxygenated ACSF and cultures were allowed to recover in the roller incubator for at least 1 h. OTCs were imaged under constant perfusion with 32  $^{\circ}\text{C}$  oxygenated ACSF, at a rate of 3–5 ml per min. The imaging setup is based on a custom-build two-photon laser scanning microscope with a Ti:sapphire laser system (Spectra Physics, Mountain View, CA, USA). This system provides a mode-locked laser light (pulse width < 100 fs, 80 MHz, center wavelength 790 nm)

and is connected to a scanning setup (Sutter Instruments, Lambrecht/Pfalz, Germany) with a water-immersion objective ( $\times 20$ , 0.8 NA, Zeiss, Oberkochen, Germany). Image analysis and acquisition of data were done with MacBiophotonics ImageJ software, MatLab 6.5 and ScanImage 3.0 [38]. For confocal calcium imaging, single neurons transfected with GCaMP6m alone or together with effector proteins (KAR subunits, TTBK2-KD) were recorded earliest after a 2-day period of overexpression. At the day of recording, the culture medium was replaced by oxygenated ACSF with multiple washing steps. After recovery (for at least 1 h in the incubator), cultures were imaged using a Leica TCS SP5 confocal microscope (Leica, Mannheim, Germany) with a  $\times 10$  objective at 1400 Hz and 3 frames/s. The normalization to the mean fluorescence intensities ( $\Delta F/F^0$ ) was done in order to allow comparison of data from several experiments. Z-stacks of various sizes (depending on culture thickness, but all spaced by 1  $\mu\text{m}$  steps) of neurons stained for the overexpressed fluorophore-tagged receptor subunits (GluK2(R)-pEGFP or GluA2(R)i-pEYFP, respectively) were obtained with  $\times 10$  objective at  $1024 \times 1024$  pixels. Maximum projections of images were assessed using Fiji/ImageJ [39] and enhanced for contrast and brightness only when used for qualitative image preparation.

The basal levels of activity do vary between batches and even between sister cultures from the same animal. One factor is the degree of maturity of the cortex at the time of explantation. Smaller litters are advanced compared to large litters as published [40]. Further, it is known that neurons cope in a very individual manner with OGB loading or GCaMP overexpression—these sensors can interfere with neuronal physiology which might also be one factor to influence the basal levels of activity. Therefore, we always test our treatment groups against sister cultures made from the animals from the same litter (1 batch/1 culture preparation). Further, as development advances, the levels of activity at different time points vary—in fact, the control traces show a natural increase in spontaneous activity (to be seen, e.g., in Fig. 1). Last but not least, depending on how many recordings from DIV 7 or DIV 10 finally ended in the pool, the frequencies vary between 5 and 12 calcium events per 5 min in the controls.

### Assessment of Relative Fluorescence Intensities Along Dendrites

The analysis of the differential expression patterns of each fluorophore-tagged receptor in the presence or absence of TTBK2-KD overexpression (Supplementary Fig. 2) was done as described [41]. In brief, using the Simple Neurite Tracer plugin for ImageJ, multiple randomly chosen dendritic segments of each neuron were analyzed in 5  $\mu\text{m}$  bins. Dendrites were identified by ALEXA-488 fluorescence originating from

the immunostained GFP located within the C-terminal domain of the given receptor. Fluorescence intensity was normalized to maximal intensity of each dendrite. The length of each dendrite analyzed was set from 0 to 1.0 by piecewise linear interpolation to normalize the line profile distance. Subsequently, the obtained interpolated data were pooled, and the mean  $\pm$  s.e.m was plotted against normalized distance.

### Statistical Analysis

Statistical analysis was performed using SigmaPlot12 (SPSS Inc., Chicago, USA). For all data, non-parametric ANOVA on Ranks tests with corrections for multiple testing when appropriate (Bonferroni or Dunn's test) was conducted followed by Mann-Whitney rank sum tests. Graphs were created with SigmaPlot12 (SPSS Inc., Chicago, USA).

## Results

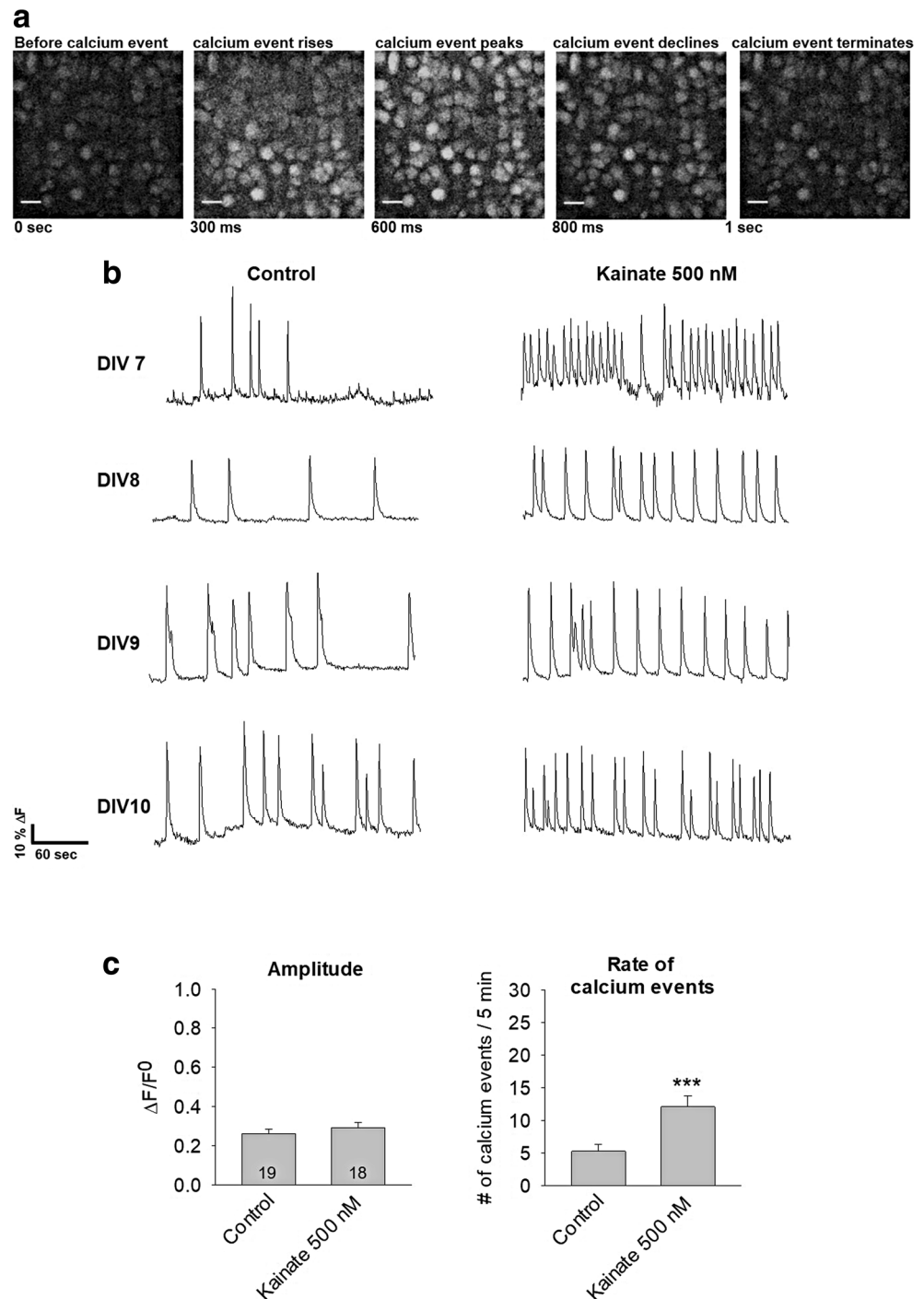
### A Low Dose of Kainate Is Sufficient to Increase Network Activity in OTCs

One major role of functional KARs is to regulate network activity [42]. To confirm if the KARs are functionally expressed in OTCs, we monitored neuronal activity with two-photon calcium imaging in the absence and presence of kainate (Fig. 1) in OTCs aged DIV 7–10. Wash-in of 500 nM kainate (low kainate concentrations are known to activate only KARs [43]) increased network activity at every developmental time point tested (Fig. 1a, b; Supplementary Fig. 4A). While the amplitudes of spontaneous calcium events were unchanged, the rate of events was significantly increased (Fig. 1c, Supplementary Fig. 4A). This confirmed that KARs are functionally expressed during the time window tested, and that 500 nM kainate is sufficient to enhance network activity.

### Chronic Kainate Treatment Enhances Maturation of Supragranular Pyramidal Cells

Next, we tested if the low dose of kainate can influence dendritic growth. OTCs were transfected with EGFP at DIV 5 and treated once daily either with water as control or 500 nM kainate in water from DIV 6–10, medium was exchanged every second day. Kainate treatment resulted in a significant increase of apical dendrite length and branching of layer II/III pyramidal cells, but failed to promote dendritic growth of layer VI pyramidal cells (Table 1A). In addition, the basal dendrites of both cell types were unaffected by the kainate treatment. Considering interneurons, kainate failed to elicit dendritic growth (Table 1B). This suggested that the KAR-

**Fig. 1** Kainate increases spontaneous network activity in OTCs. **a** Representative images of a two-photon recording from an individual OTC (DIV 8) showing the rise, peak, and decline of a spontaneous calcium event. **b** Representative traces of spontaneous calcium events (expressed as  $\Delta F/F^0$ ) at DIV 7–10 in the absence (control) and after wash-in of 500 nM kainate. **c** Quantitative analysis (mean  $\pm$  s.e.m.) of amplitudes and frequencies of spontaneous calcium events before (control) and after wash-in of kainate (DIV 7–10 recording, data pooled). Note that DIV 5–10 is the time window for the analysis of dendritic growth. Numbers of analyzed OTCs are given in the bars. \*\*\*,  $P < 0.001$  for treatment versus control group. Scale bars 20  $\mu\text{m}$



induced network activity promotes dendritic maturation in a cell class- and compartment-specific manner.

### Acute ATPA Treatment Reduces Network Activity in OTCs

In order to investigate if interneurons in OTCs express functional GluK1-containing KARs during the early postnatal time window, we recorded calcium events in the absence or presence of

1  $\mu\text{M}$  ATPA, a potent GluK1-selective agonist [44]. Activating interneurons with ATPA has been reported to increase the GABAergic inhibition in pyramidal neurons [44–48] resulting in a reduction of network activity. As expected, the rate of spontaneous calcium events significantly decreased in the presence of ATPA, and this effect was reversed after washout (Fig. 2a, b); amplitudes were not affected. These observations suggested that interneurons in OTCs express functional GluK1-containing KARs which can be activated by ATPA.

**Table 1** Quantitative morphometric analysis of kainate-treated pyramidal cells and interneurons (A). Mean  $\pm$  s.e.m. of apical and basal dendritic length and segment number of pyramidal cells from layer II/III and layer V/VI treated with water as control or 500 nM kainate, respectively. ADL, apical dendritic length ( $\mu\text{m}$ ); BDL, mean basal dendritic length ( $\mu\text{m}$ ). (B) Mean  $\pm$  s.e.m. of dendritic length and

segment numbers of interneurons treated with water as control or 500 nM kainate, respectively. MDL, mean dendritic length ( $\mu\text{m}$ ); MDS, mean dendritic segments; PD, number of primary dendrites. The number of reconstructed cells per group is given in (n). In this and the following tables, values in *italic* followed by *P* values indicate significant differences to the control condition.

A. Kainate-treated pyramidal cells				
Treatment	Pyramidal cells in layers II/III		Pyramidal cells in layers V/VI	
	ADL ( <i>n</i> )	BDL	ADL ( <i>n</i> )	BDL
	Segments	Segments	Segments	Segments
H <sub>2</sub> O control	1053 $\pm$ 48 (81)	212 $\pm$ 13	1021 $\pm$ 43 (93)	252 $\pm$ 30
	28.7 $\pm$ 1.4	6.4 $\pm$ 0.3	25.1 $\pm$ 1.4	6.7 $\pm$ 0.3
Kainate 500 nM	<i>1289 <math>\pm</math> 49 (130), <i>P</i> = 0.003</i>	245 $\pm$ 13	1054 $\pm$ 34 (124)	248 $\pm$ 11
	<i>37.7 <math>\pm</math> 1.5, <i>P</i> &lt; 0.001</i>	8.1 $\pm$ 0.4	23 $\pm$ 0.9	6.5 $\pm$ 0.3
B. Kainate-treated interneurons				
Treatment	MDL ( <i>n</i> )	MDS ( <i>n</i> )	PD	
H <sub>2</sub> O control	394 $\pm$ 20 (63)	9.3 $\pm$ 0.7	4.7 $\pm$ 0.2	
Kainate 500 nM	377 $\pm$ 23 (66)	9.5 $\pm$ 1	4.6 $\pm$ 0.2	

### Pharmacological Treatment Targeting of GluK1 Affects Dendritic Maturation of Interneurons

Since interneurons did not display an enhanced dendritic growth upon kainate treatment, we applied the more potent GluK1-agonist ATPA at 1  $\mu\text{M}$  to OTCs from DIV 6 to 10. ATPA failed to alter the morphology of pyramidal cells (Table 2A). Interestingly, ATPA-treated interneurons displayed a significant increase in mean dendritic length (MDL) by 17.3% (Table 2B; for representative ATPA-treated interneurons, see Fig. 6c). This observation suggested that the GluK1 subunit can elicit dendritic elongation in interneurons. By contrast, when the GluK1 antagonist UBP 310 (1  $\mu\text{M}$ ) was applied, the MDL was significantly decreased by 28.17% (Table 2C). Together, the two experiments suggested a role of GluK1 for dendritic growth in interneurons.

### Overexpression of GluK2(Q) and GluK2(R) Enhances the Activity of Individual Neurons

It has been reported that the GluK2 subunit is important for regulating cell excitability and network activity [43, 49–53]. In order to test if an enhanced expression of GluK2 leads to an enhanced activity of the neurons, we transfected the genetically encoded calcium sensor GCaMP6m alone as control or together with either GluK2(Q) or GluK2(R), respectively. Only pyramidal cells with a clearly identifiable axon were recorded (Fig. 3a). Confocal calcium imaging of individual transfectants revealed that the frequency of spontaneous calcium events was enhanced in neurons overexpressing GluK2(Q) or GluK2(R), compared to controls at DIV 7–10 (Fig. 3b, c). Amplitudes were not different (Fig. 3c). This suggested that GluK2 is, independent of its editing status, a regulator of excitability and that neurons overexpressing

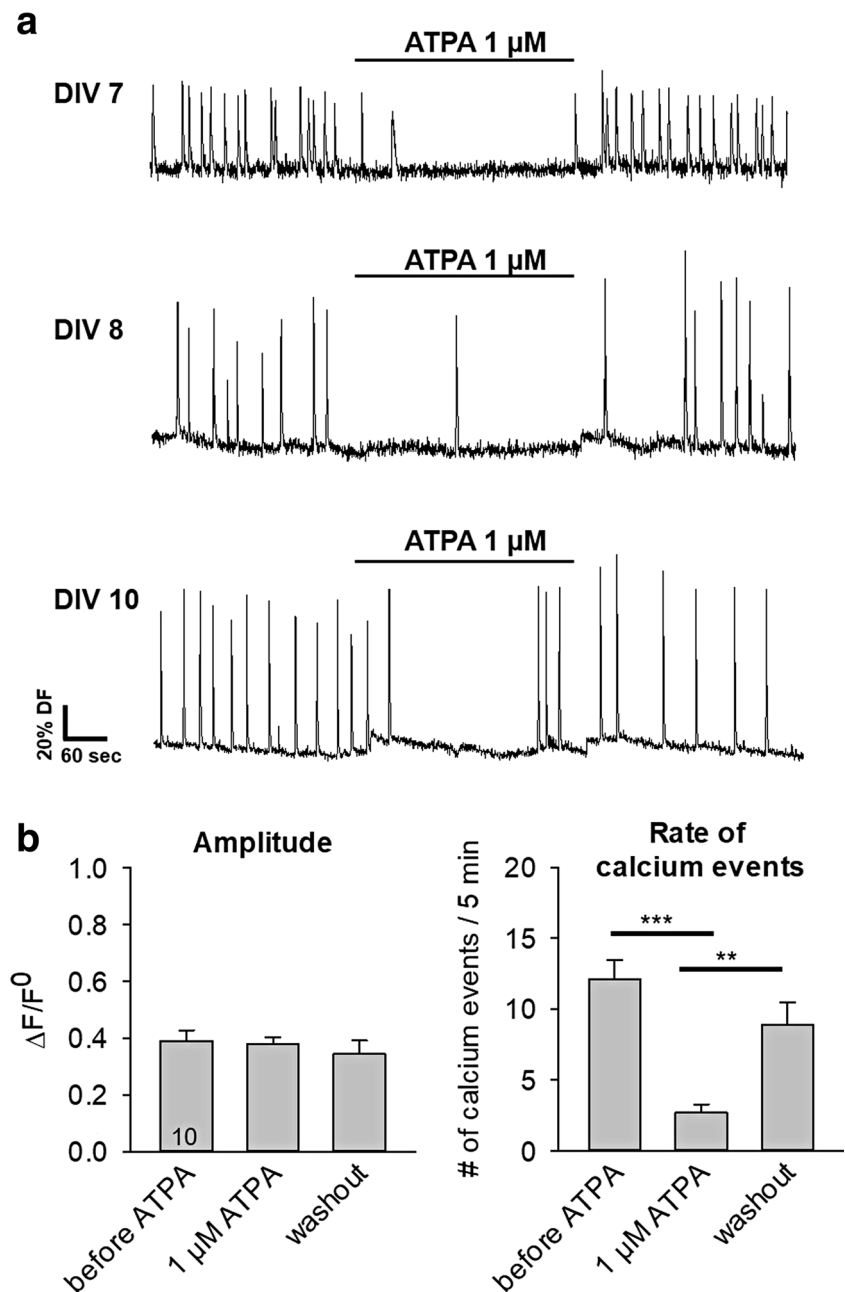
GluK2 are significantly more active than age-matched wild-type neurons.

### TTBK2-KD Decreases Spontaneous Activity of Individual Neurons

A recent study has shown that tau-tubulin kinase-2 (TTBK2) can reduce GluK2 surface expression in a Rab5-dependent manner, and this function is independent of its kinase activity [54]. We therefore employed TTBK2 as a brain-derived enzymatic tool to elicit via its overexpression a partial knockdown of endogenous GluK2 in individual cells. In order to avoid potential effects mediated by the kinase domain, we used the kinase-dead TTBK2 mutant (TTBK2-KD) for the experiments because its only known function is to promote GluK2 endocytosis [54]. We first overexpressed TTBK2-KD together with GFP-tagged GluK2 subunits and assessed the relative fluorescence patterns along arbitrarily selected dendritic segments (Supplementary Fig. 2). When coexpressed with TTBK2-KD, the distribution of GluK2(R)-EGFP resembled a vesicular pattern compared to GluK2(R)-EGFP alone (Supplementary Fig. 2A, B), and concurrently, the relative fluorescence along dendrites was significantly decreased (Supplementary Fig. 2C). As a control, we tested if TTBK2-KD could affect the distribution of GluA2(R)-i-EYFP in a similar fashion, and this was not the case (Supplementary Fig. 2D–F). If the endogenously expressed GluK2 subunits are required for neuronal activity, an overexpression of TTBK2-KD and the resulting reduction of surface GluK2 should decrease the activity of the transfected neurons. Intriguingly, neurons transfected with TTBK2-KD displayed about 50% less spontaneous calcium events compared to age-matched wild-type cells recorded in sister cultures (Fig. 4a, b); amplitudes were not different. In addition, TTBK2-

**Fig. 2** ATPA reduces network activity in OTCs. **a**

Representative traces of spontaneous calcium events (expressed as  $\Delta F/F^0$ ) at ages indicated in the absence or presence of 1  $\mu\text{M}$  ATPA. **b** Quantitative analysis (mean  $\pm$  s.e.m.) of amplitudes and frequencies of spontaneous calcium events in ATPA-treated OTCs (DIV 7–10 recording data pooled), showing that ATPA does not influence the amplitudes but decreases the rate of spontaneous calcium events. Numbers of analyzed OTCs are given within bars. \*\*\*,  $P < 0.001$  for 1  $\mu\text{M}$  ATPA versus control (= before ATPA); \*\*,  $P = 0.001$  for 1  $\mu\text{M}$  ATPA versus washout



KD transfectants were significantly less sensitive to kainate-induced excitotoxicity determined by dendritic injury assay (Supplementary Fig. 1D, E). These observations provided further evidence that GluK2 is important for promoting activity during the early postnatal time window.

### GluK2 Transfectants Increase Network Activity in OTCs

Next, we asked if the comparatively few GluK2-overexpressing neurons generated by biolistic transfection in every OTC can transmit their enhanced activity to neighboring wild-type neurons. OTCs were transfected at DIV 5 with

either EGFP alone or with EGFP plus one of the GluK2 editing variants. To monitor activity of wild-type neurons, we used the calcium dye OGB. For recording, we selected in every OGB-loaded OTC those areas of interest which were void of EGFP-expressing or EGFP/GluK2-expressing neurons, in order to only record calcium events from wild-type cells not overexpressing GluK2 (five arbitrarily selected somata per ROI). Interestingly, two-photon calcium imaging revealed that wild-type cells in OTCs harboring GluK2 transfectants display significantly higher frequencies of calcium events than age-matched wild-type cells from OTCs harboring only EGFP transfectants (Fig. 5a, b). Amplitudes remained unchanged (Fig. 5b). These observations suggested

**Table 2** Quantitative morphometric analysis of ATPA-treated pyramidal cells and interneurons (A). Mean  $\pm$  s.e.m. of apical and basal dendritic length and segment number of pyramidal cells from layer II/III and layer V/VI treated with water as control or 1  $\mu$ M ATPA, respectively. ADL, apical dendritic length ( $\mu$ m); BDL, mean basal dendritic length ( $\mu$ m). (B) Mean  $\pm$  s.e.m. of dendritic length and segment numbers of

interneurons treated with water as control or 1  $\mu$ M ATPA, respectively. (C) Mean  $\pm$  s.e.m. of dendritic length and segment numbers of interneurons treated with DMSO as control or 1  $\mu$ M UBP 310, respectively. MDL, mean dendritic length ( $\mu$ m); MDS, mean dendritic segments; PD, number of primary dendrites. The number of reconstructed cells per group is given in (*n*)

A. ATPA-treated pyramidal cells				
Treatment	Pyramidal cells in layers II/III		Pyramidal cells in layers V/VI	
	ADL ( <i>n</i> )	BDL	ADL ( <i>n</i> )	BDL
	Segments	Segments	Segments	Segments
H <sub>2</sub> O control	1133 $\pm$ 50 (62)	213 $\pm$ 14	975 $\pm$ 55 (41)	238 $\pm$ 22
	31.6 $\pm$ 1.5	6.6 $\pm$ 0.5	22.6 $\pm$ 1.4	6.1 $\pm$ 0.5
ATPA 1 $\mu$ M	1192 $\pm$ 42 (93)	243 $\pm$ 15	1053 $\pm$ 38 (57)	285 $\pm$ 18
	30 $\pm$ 1.3	6.9 $\pm$ 0.3	23 $\pm$ 1.2	6.8 $\pm$ 0.4
B. ATPA-treated interneurons				
Treatment	MDL ( <i>n</i> )	MDS ( <i>n</i> )	PD	
H <sub>2</sub> O control	341 $\pm$ 16 (54)	7 $\pm$ 0.3	4.1 $\pm$ 0.2	
ATPA 1 $\mu$ M	400 $\pm$ 15 (89), <i>P</i> = 0.017	7.7 $\pm$ 0.3	4.4 $\pm$ 0.2	
C. UBP 310-treated interneurons				
Treatment	MDL ( <i>n</i> )	MDS ( <i>n</i> )	PD	
Control + DMSO	529 $\pm$ 42 (28)	9.4 $\pm$ 0.9	4.9 $\pm$ 0.3	
UBP 310 1 $\mu$ M	380 $\pm$ 18 (27), <i>P</i> = 0.007	6.7 $\pm$ 0.4, <i>P</i> = 0.02	4.4 $\pm$ 0.4	

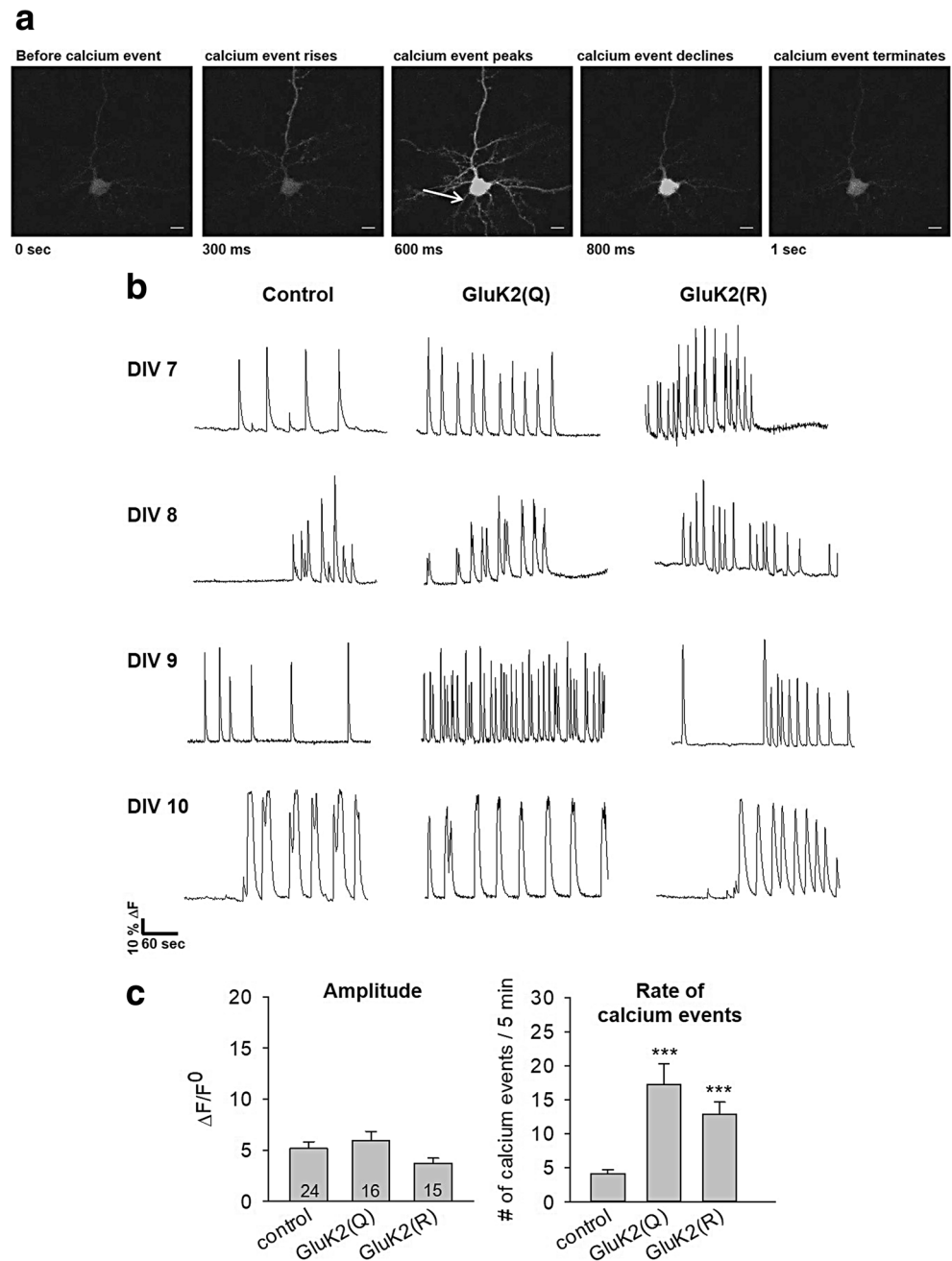
that GluK2-overexpressing neurons display a “pacemaker-like behavior” which drives the activity in the organotypic neuronal network. This is in line with a role of the GluK2 subunit in promoting network activity. Further, the effect was independent of the editing status of GluK2. We also tested if the wild-type network is affected by cells overexpressing GluK1 and found that both GluK1 editing variants failed to alter amplitudes and frequencies (Fig. 5c, Supplementary Fig. 4B).

### Selected GluK Subunits Promote Dendritic Growth in a Cell Class- and Compartment-Specific Manner

To test their influence on dendritic growth, various KAR subunit editing variants were overexpressed from DIV 5 to 10. To test if an overexpression of transfected KAR subunits occurred, we transfected neurons with GluK2(R) containing a C-terminal GFP-tag. Confocal imaging revealed that neurons expressed clearly detectable quantities of GFP-tagged GluK2(R) protein and that the protein subunit was dispersed throughout the neurites (Fig. 6a; Supplementary Fig. 2A). This confirms reports that transfection with GluK2 in CA3 pyramidal cells leads to a labeling of the somatodendritic compartment [55]. Evidence that functional GluK subunit overexpression had been elicited was determined by dendritic injury assays which reported that the two GluK1 and the two GluK2 variants confer a significantly higher sensitivity to kainate (see Supplementary Fig. 1A–C).

Regarding dendritic maturation, both GluK2(R) and GluK2(Q) were able to increase elongation and branching of apical dendrites in layer II/III pyramidal cells (Table 3A; for representative pyramidal cells, see Fig. 6b). Further, GluK2(Q) and GluK2(R) increased the dendritic complexity of layer II/III apical dendrites as revealed by Sholl analysis (Supplementary Fig. 3A). For basal dendrites of layer II/III pyramidal cells, length and segmentation were not significantly different when tested with an ANOVA on ranks (Table 3A). However, the Sholl analysis revealed that in the basal dendrites of GluK2(Q), but not GluK2(R) overexpressing pyramidal cells, the branching was increased in the proximal parts of the dendrites (Supplementary Fig. 3B). GluK1(Q) and GluK1(R) as well as the high-affinity subunit GluK5 failed to change the morphology of pyramidal cells (Table 3A). In another experiment, we examined if the augmented network activity induced by GluK2(R) transfectants is sufficient to promote dendritic growth in wild-type neurons overexpressing mCherry only in the same OTC. Interestingly, the apical dendrites of layer II/III pyramidal cells of these wild-type neurons displayed an increase in elongation and branching in a similar compartment-specific fashion as GluK2(R) transfectants (Table 3B). In interneurons, both, GluK2(Q) and GluK2(R) were able to enhance dendritic elongation, but not branching. Interestingly, the two editing variants of GluK1, known to be enriched in interneurons [17, 56, 57], indeed promoted dendritic elongation and branching only in interneurons (Table 3C; for representative GluK1-overexpressing interneurons, see Fig. 6c). Overexpression of

**Fig. 3** GluK2(Q) and GluK2(R) both increase spontaneous activity of transfected neurons. **a** Representative images of a confocal recording from an individual neuron (DIV 8) expressing GCaMP6 showing the rise, peak, and decline of a single spontaneous calcium event. Only cells with clearly identifiable axons were considered for recording. Arrow points to axon. **b** Representative traces of spontaneous calcium events (expressed as  $\Delta F/F^0$ ) at ages indicated from cells overexpressing GCaMP6 only as control or coexpressing GCaMP6 with the GluK subunit indicated. **c** Quantitative analysis (mean  $\pm$  s.e.m.) of amplitudes and frequencies of spontaneous calcium events from cells expressing GCaMP6 only as control or coexpressing GCaMP6 with the GluK subunit indicated (DIV 7–10 recording data pooled). GluK2(Q) and GluK2(R) both increase the rate of spontaneous calcium events displayed by single transfectants in the time window permitted for dendritic growth. Numbers of analyzed cells are given within bars. \*\*\*,  $P < 0.001$  for treatment versus control group. Scale bars 25  $\mu$ m



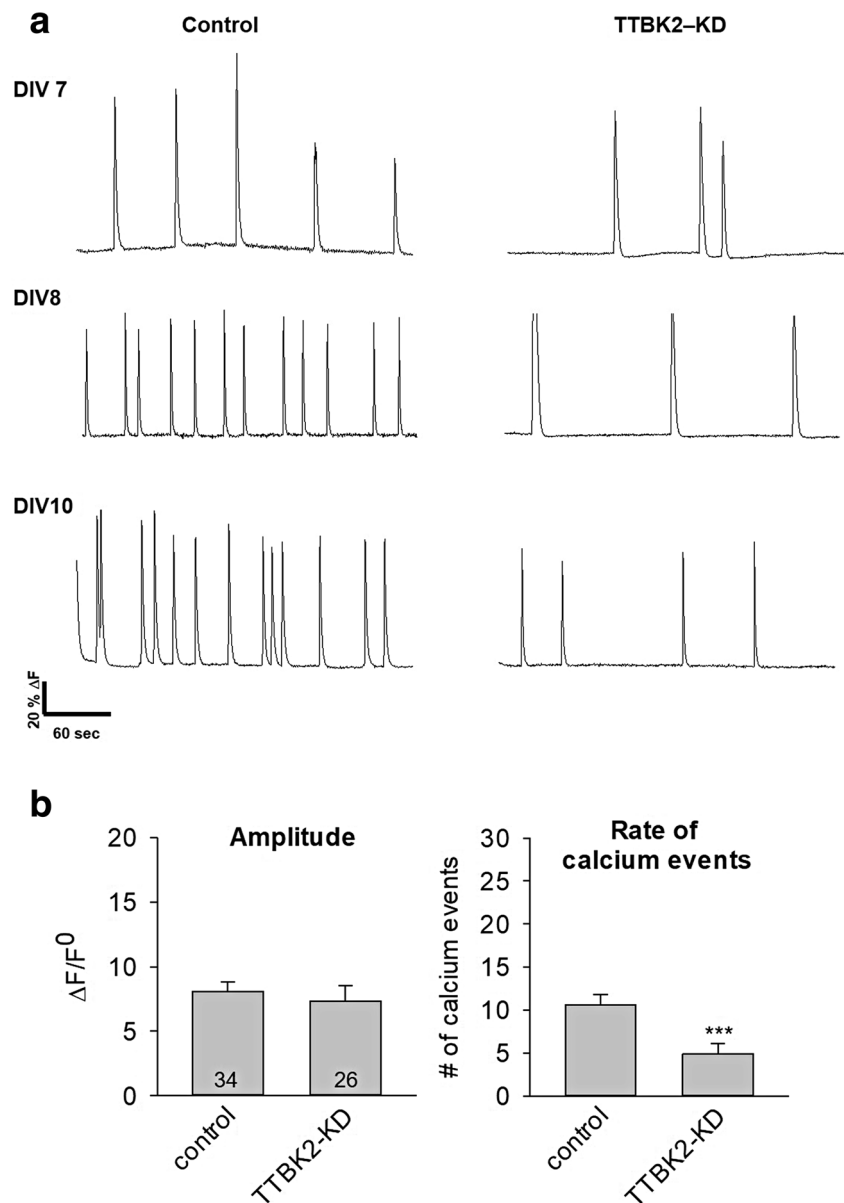
GluK5 failed to enhance dendritic growth of interneurons (Table 3C). Taken together, the data suggested that KARs contribute in a very distinct manner to dendritic maturation of neocortical neuron types.

### NMDARs and VGCCs But Not AMPARs Are Required for KAR-Mediated Dendritic Growth

It has been previously reported that overexpressing either selected AMPARs of the flip splice variant or trafficking-competent type-I TARPs can promote pyramidal cell dendritic growth. Physiologically, the overexpression correlates with an increase

in amplitude, but not rate, of spontaneous calcium events [9, 10]. The enhanced cationic influx in turn activates NMDARs and VGCCs, and indeed those channels were required downstream of AMPARs [9]. In the present study, the GluK2 overexpression increased the frequency of calcium events which could also result in an enhanced activation of NMDARs and VGCCs. To examine if NMDARs and VGCCs also act as downstream mediators of the KAR-induced dendritic growth, we treated GluK2(R)-overexpressing neurons with the NMDAR antagonist APV and the L-type VGCC blocker nifedipine. Indeed, APV and nifedipine abolished the growth-promoting action of GluK2(R) in pyramidal cells and interneuron (Table 4A, C). This

**Fig. 4** TTBK2-KD-transfected neurons display decreased spontaneous activity. **a** Representative traces of calcium events (expressed as  $\Delta F/F^0$ ) at ages indicated from cells overexpressing GCaMP6 only as control or coexpressing GCaMP6 with TTBK2-KD. **b** Quantitative analysis (mean  $\pm$  s.e.m.) of amplitudes and frequencies of spontaneous calcium events from cells expressing GCaMP6 only as control or coexpressing GCaMP6 with TTBK2-KD (DIV 7–10 recording data pooled). In the presence of TTBK2-KD, transfected neurons display a decreased rate of spontaneous calcium events. Numbers of analyzed cells are given within bars. \*\*\*,  $P < 0.001$  for treatment versus control group



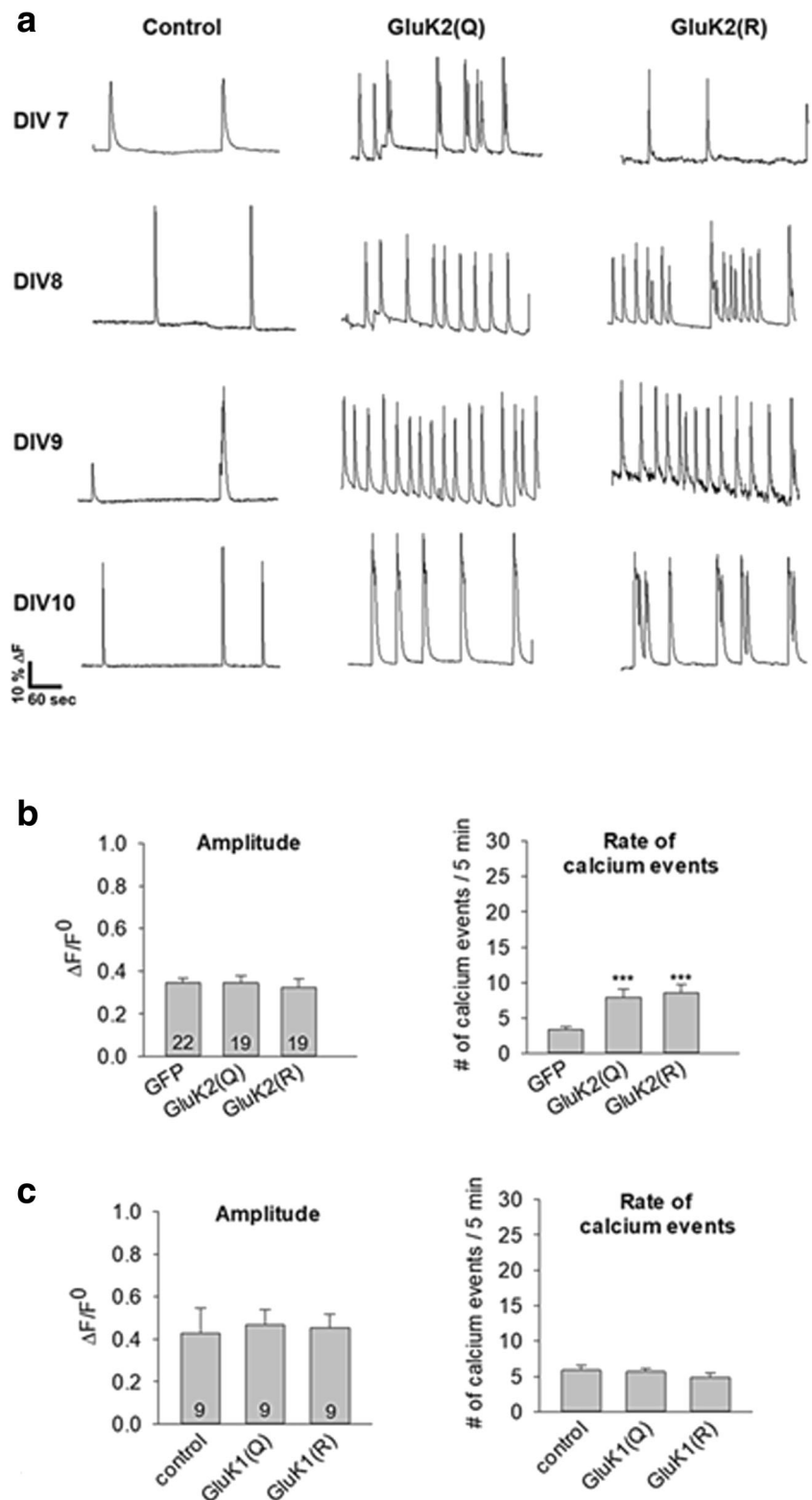
implicated that KARs, similar to AMPARs, employ downstream signaling of NMDARs and VGCCs to promote dendritic growth. Neurons expressing EGFP only that were treated with APV or nifedipine were not significantly affected (Table 4B). Next, we asked if KARs act upstream of AMPARs. For this, we tested the GluK2(R)-mediated effect in the presence of 1  $\mu$ M GYKI 47261, a selective AMPAR antagonist. Interestingly, the effect of GluK2(R) overexpression was not abolished by GYKI 47261 (Table 5), suggesting that GluK2 exerts its effects independent from AMPARs.

### TTBK2-KD Transfectants Display a Reduction in Apical Dendrite Branching

TTBK2-KD-transfected neurons displayed an internalization of endogenous GluK2 and a decreased spontaneous activity

(Fig. 4). We asked if this could affect dendritic maturation. Indeed, a DIV 5–10 overexpression of TTBK2-KD resulted in slightly, but not significantly shorter apical dendrites (9.7% shorter for layer II/III pyramidal cells; 11.6% shorter for layer VI pyramidal cells; Table 6A). However, there was a significant reduction in the apical dendrite branching of both cell classes (15.4% fewer segments for layer II/III pyramidal cells; 16.3% fewer segments for layer VI pyramidal cells). Accordingly, Sholl analysis of layer II/III apical dendrites revealed that TTBK2-KD overexpression resulted in a significant reduction of dendritic complexity (Supplementary Fig. 3C). Interneurons remained unaffected by the overexpression of TTBK2-KD (Table 6B). This observation suggested that a reduction of surface GluK2 and the resulting decrease in excitability are sufficient to impair the morphological maturation of pyramidal cells.

**Fig. 5** GluK2(Q) and GluK2(R) transfectants both increase network activity in OTCs. **a** Representative traces of spontaneous calcium events in wild-type neurons loaded with OGB-1 AM (expressed as  $\Delta F/F^0$ ) at ages indicated in the absence or presence of GluK2(Q) or GluK2(R) transfectants within the same OTC. Control OTCs contained EGFP-expressing neurons only. Areas of interest in OTCs containing EGFP + GluK2(Q) or EGFP + GluK2(R) transfectants were randomly placed in sections that did not contain EGFP signals from transfectants. **b** Quantitative analysis (mean  $\pm$  s.e.m.) of amplitudes and frequencies of spontaneous calcium events from OGB-1 AM-loaded wild-type cells in the absence or presence of GluK1(Q) or GluK1(R) transfectants within the same OTC (DIV 7–10 recording data pooled). **c** Quantitative analysis (mean  $\pm$  s.e.m.) of amplitudes and frequencies of spontaneous calcium events from OGB-1 AM-loaded wild-type cells in the absence or presence of GluK2(Q) or GluK2(R) transfectants within the same OTC (DIV 7–10 recording data pooled), showing that GluK2(Q) and GluK2(R) transfectants do not influence the amplitudes of wild-type neurons but increase the rate of spontaneous calcium events in those cells. Numbers of analyzed OTCs are given within bars. \*\*\*,  $P < 0.001$  for treatment versus control group

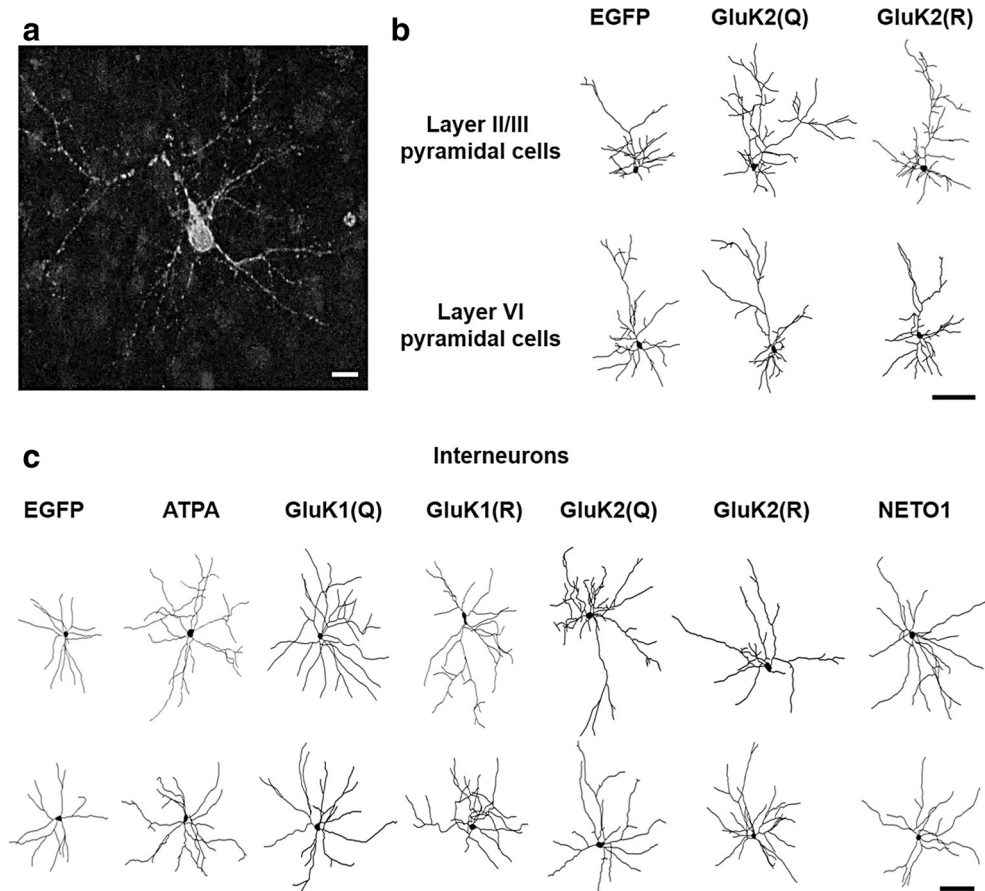


### NETO1 Specifically Promotes Dendritic Growth of Interneurons

Trafficking-competent type-I TARPs promote dendritic maturation of pyramidal cells due to an increased surface delivery

of AMPARs [10]. Interestingly, all of the TARPs failed to promote dendritic growth of interneurons, and reasons for this observation have remained elusive. NETOs are auxiliary subunits for KARs and modulate channel kinetics [58, 59]. Although their role in trafficking KARs is still under debate

**Fig. 6** Representative pyramidal cells and interneurons at DIV 10. **a** Confocal image (z-stack) of a neuron (DIV 8) overexpressing GluK2(R) with a c-terminal GFP-tag (GluK2(R)-pEGFP N1). Scale bar 20  $\mu\text{m}$ . **b** Representative NeuroLucida reconstructions of pyramidal cells transfected with plasmids encoding EGFP alone as control or together with the indicated GluK subunit. Scale bar 100  $\mu\text{m}$ . **c** Representative NeuroLucida reconstructions of interneurons. Cells were transfected with EGFP as control, treated with 1  $\mu\text{M}$  ATPA from DIV 5–10, or cotransfected with the GluK or NETO subunit indicated. Scale bar 100  $\mu\text{m}$



[60], a recent study has revealed that NETO1 is important for GluK1 surface expression in interneurons [61]. Therefore, we overexpressed NETO1 and NETO2 from DIV 5 to 10 and assessed their influence on dendritic maturation. Both NETOs failed to change the morphology of pyramidal cells (Table 7A). Strikingly, NETO1 significantly enhanced dendritic elongation of interneurons (Table 7B; for representative NETO1-overexpressing interneurons, see Fig. 6b). NETO2 failed to do this. In another experiment, NETO1 overexpressing interneurons were kept under the GluK1 antagonist UBP 310 [1  $\mu\text{M}$ ], and this prevented the effect on dendritic growth in interneurons (Table 7C). These observations suggested that NETO1 can specifically promote dendritic maturation in interneurons, most likely by increasing surface expression of GluK1-containing KARs.

### PKC or PKA Inhibitors Prevent the Network-Promoting Effect of Kainate

We initially tried to test if inhibition of PKC or PKA could influence the dendritogenic effects of KARs. However, when OTCs were kept chronically under calphostin C (PKC blocker, 1  $\mu\text{M}$ ) from DIV 5 to 10, the cells eventually all died, making it impossible to test

whether KAR-mediated dendritic growth would be affected by PKC inhibition. The experiments with H89 (PKA blocker, 10  $\mu\text{M}$ ) ended up in the same way. Alternatively, we tested if these blockers would affect the influence of 500 nM kainate on network activity. For this, OTCs were loaded as described with OGB and recorded on DIV 8. After the baseline activities could as expected be augmented by 500 nM kainate, the blockers were applied for 30 min. Subsequently, blockers were washed out with ACSF containing 500 nM kainate for 10 min before activity was recorded. The network activity was almost completely abolished after the treatment with either calphostin C or H89, respectively. Even the presence of 500 nM kainate following the washout failed to restore the activity (Fig. 7a). The amplitudes and the rate of spontaneous calcium events were significantly reduced after treatment with calphostin C or H89, respectively (Fig. 7b). Network activity did not recover within 20 min before the recording was terminated (not shown). This confirmed that both PKC and PKA are involved in the kainate-mediated increase in cellular excitability and network activity [20–22, 51, 52]. To this end, we can only speculate that the growth-promoting effects of KARs might involve activation of PKC and/or PKA.

**Table 3** Quantitative morphometric analysis of KAR-mediated effects on pyramidal cells and interneurons (A). Mean  $\pm$  s.e.m. of apical and basal dendritic length and segment number of pyramidal cells from layer II/III and layer V/VI overexpressing the indicated GluK subunits or living within GluK2(R) transfectants within the same network. For “GluK2 Q/R,” ANOVA on ranks vs “control for GluK2” with Dunn’s correction for multiple testing was performed followed by Mann-Whitney *U* tests. *P* values are given. ADL, apical dendritic length ( $\mu$ m); BDL, mean basal dendritic length ( $\mu$ m). (B) Mean  $\pm$  s.e.m. of apical and basal dendritic length and segment number of “wild-type” pyramidal cells from layer II/III neurons expressing mCherry only within a network containing GluK2(R) transfectants. (C). Mean  $\pm$  s.e.m. of dendritic length and segment numbers of interneurons overexpressing the indicated GluK subunits. For “GluK1 Q/R,” ANOVA on ranks vs “control for GluK1” with Dunn’s correction for multiple testing was performed followed by Mann-Whitney *U* tests. For “GluK2 Q/R,” ANOVA on ranks vs “control for GluK2” with Dunn’s correction for multiple testing was performed followed by Mann-Whitney *U* tests. *P* values are given. MDL, mean dendritic length ( $\mu$ m); MDS, mean dendritic segments; PD, number of primary dendrites. The number of reconstructed cells per group is given in (*n*)

A. Pyramidal cells overexpressing KARs				
Condition	Pyramidal cells in layers II/III		Pyramidal cells in layers V/VI	
	ADL ( <i>n</i> ) Segments	BDL Segments	ADL ( <i>n</i> ) Segments	BDL Segments
Control for GluK1	1104 $\pm$ 45 (45)	218 $\pm$ 13	1102 $\pm$ 40 (90)	300 $\pm$ 14
GluK1(Q)	29.2 $\pm$ 1.6	6 $\pm$ 0.3	18.9 $\pm$ 0.7	5.8 $\pm$ 0.2
GluK1(R)	1180 $\pm$ 47 (46)	261 $\pm$ 18	1134 $\pm$ 58 (64)	284 $\pm$ 15
GluK1(R)	31.9 $\pm$ 1.7	7.6 $\pm$ 0.5	21.5 $\pm$ 1	5.9 $\pm$ 0.3
Control for GluK2	1211 $\pm$ 53 (40)	276 $\pm$ 20	1150 $\pm$ 58 (81)	282 $\pm$ 14
GluK2(Q)	29.2 $\pm$ 1.9	7.5 $\pm$ 0.5	23 $\pm$ 1.2	6.6 $\pm$ 0.3
GluK2(Q)	1082 $\pm$ 40 (90)	224 $\pm$ 11	996 $\pm$ 39 (88)	286 $\pm$ 17
GluK2(Q)	33.6 $\pm$ 1.4	7.6 $\pm$ 0.3	25.2 $\pm$ 1.3	7.7 $\pm$ 0.3
GluK2(R)	1330 $\pm$ 76 (52), <i>P</i> = 0.005	249 $\pm$ 13	1099 $\pm$ 37 (91)	288 $\pm$ 12
GluK2(R)	42.4 $\pm$ 2.7, <i>P</i> = 0.008	8.8 $\pm$ 0.4	26.9 $\pm$ 1.2	8.2 $\pm$ 0.2
GluK2(R)	1327 $\pm$ 48 (93), <i>P</i> < 0.001	265 $\pm$ 13	1140 $\pm$ 44 (75)	297 $\pm$ 20
GluK2(R)	40.3 $\pm$ 1.5, <i>P</i> < 0.001	8.6 $\pm$ 0.4	23.3 $\pm$ 1.2	7.8 $\pm$ 0.4
Control for GluK5	1112 $\pm$ 96 (20)	232 $\pm$ 26	1028 $\pm$ 37 (29)	235 $\pm$ 21
GluK5	28.7 $\pm$ 2.4	6.7 $\pm$ 0.7	23.2 $\pm$ 1.7	5.7 $\pm$ 0.4
GluK5	1075 $\pm$ 84 (18)	244 $\pm$ 28	930 $\pm$ 44 (28)	261 $\pm$ 25
GluK5	31.2 $\pm$ 9.5	7.7 $\pm$ 0.9	20.8 $\pm$ 1.3	6.4 $\pm$ 0.6
B. “Wild-type” pyramidal cells in network with GluK2(R) transfectants				
Without GluK2(R) in network	870 $\pm$ 118.5(13)	321 $\pm$ 38		
Without GluK2(R) in network	19.5 $\pm$ 2.3	7.8 $\pm$ 1.1		
With GluK2(R) in network	1544 $\pm$ 119.2(13), <i>P</i> < 0.001	320 $\pm$ 35		
With GluK2(R) in network	36.8 $\pm$ 3.4, <i>P</i> < 0.001	8.8 $\pm$ 0.8		
C. Interneurons overexpressing KARs				
Condition	MDL ( <i>n</i> )	MDS ( <i>n</i> )	PD	
Control for GluK1	322 $\pm$ 18 (51)	5.1 $\pm$ 0.2	5.2 $\pm$ 0.2	
GluK1(Q)	397 $\pm$ 20 (41), <i>P</i> = 0.008	7 $\pm$ 0.4, <i>P</i> < 0.001	4.9 $\pm$ 0.1	
GluK1(R)	415 $\pm$ 22 (53), <i>P</i> = 0.002	7.9 $\pm$ 0.4, <i>P</i> < 0.001	4.6 $\pm$ 0.1	
Control for GluK2	320 $\pm$ 15 (29)	7.6 $\pm$ 0.4	4.4 $\pm$ 0.1	
GluK2(Q)	415 $\pm$ 22 (45), <i>P</i> = 0.003	9.3 $\pm$ 0.6	4.8 $\pm$ 0.2	
GluK2(R)	496 $\pm$ 37 (34), <i>P</i> < 0.001	10.1 $\pm$ 0.7	4.3 $\pm$ 0.2	
Control for GluK5	409 $\pm$ 34 (15)	9.2 $\pm$ 0.9	4.6 $\pm$ 0.3	
GluK5	389 $\pm$ 36 (20)	8 $\pm$ 0.7	5.2 $\pm$ 0.3	

## Discussion

To summarize, we demonstrated that members of the kainate receptor family can contribute to differentiation of neurons in rat visual cortex, with overexpression of GluK1 and GluK2 having quite distinct cellular consequences. We report that first, GluK2 overexpression and kainate in the nanomolar range promote dendritic growth of apical dendrites in layer II/III pyramidal cells and of interneurons, whereas a subtle

decrease of endogenous GluK2 impairs dendritic growth. Second, NETO1 and GluK1 overexpression and selective GluK1 activation enhance dendritic growth only in interneurons. Third, the high-affinity subunit GluK5 does not enhance dendritic growth. Fourth, in contrast to our previous data on the neurotogenic role of AMPARs and TARPs [9, 10], the effects of GluK1 and GluK2 were independent of their editing status. Fifth, the effects concur with an increase in the frequency rather than amplitude of calcium events.

**Table 4** Quantitative morphometric analysis of pharmacologically treated cells overexpressing GluK2(R) (A). Mean  $\pm$  s.e.m. of apical and basal dendritic length and segment number of pyramidal cells from layer II/III and layer V/VI overexpressing EGFP only or together with GluK2(R) in the absence or presence of APV or nifedipine. ADL, apical dendritic length ( $\mu\text{m}$ ); BDL, mean basal dendritic length ( $\mu\text{m}$ ). For “GluK2(R) + DMSO,” “GluK2(R) + APV,” and “GluK2(R) + nifedipine,” ANOVA on ranks vs “control + DMSO” with Dunn’s correction for multiple testing was performed followed by Mann-Whitney *U* tests. *P* values are given. (B) Mean  $\pm$  s.e.m. of apical and basal dendritic length and segment number of pyramidal cells from layer II/III expressing EGFP only in the presence of absence of APV and

nifedipine. For “control + DMSO,” “control + APV,” and “control + nifedipine,” ANOVA on ranks vs “control + DMSO” with Dunn’s correction for multiple testing was performed followed by Mann-Whitney *U* tests. *P* values are given. (C) Mean  $\pm$  s.e.m. of dendritic length and segment numbers of interneurons overexpressing GluK2(R) in the absence or presence of antagonists APV or nifedipine. For “GluK2(R) + DMSO,” “GluK2(R) + APV,” and “GluK2(R) + nifedipine,” ANOVA on ranks vs “control + DMSO” with Dunn’s correction for multiple testing was performed followed by Mann-Whitney *U* tests. *P* values are given. MDL, mean dendritic length ( $\mu\text{m}$ ); MDS, mean dendritic segments; PD, number of primary dendrites. The number of reconstructed cells per group given in (*n*)

#### A. Pyramidal cells treated with APV and nifedipine

Condition	Pyramidal cells in layers II/III		Pyramidal cells in layers V/VI	
	ADL ( <i>n</i> )	BDL	ADL ( <i>n</i> )	BDL
	Segments	Segments	Segments	Segments
Control + DMSO	1046 $\pm$ 58 (38)	236 $\pm$ 17	1090 $\pm$ 97 (24)	261 $\pm$ 18
	30.6 $\pm$ 1.4	7.9 $\pm$ 0.6	24.1 $\pm$ 2.3	7.5 $\pm$ 0.5
GluK2(R) + DMSO	1430 $\pm$ 82 (34), <i>P</i> = 0.002	255 $\pm$ 18	1122 $\pm$ 83 (21)	290 $\pm$ 21
	40.8 $\pm$ 3.2, <i>P</i> = 0.008	8.3 $\pm$ 0.7	27 $\pm$ 2	8.4 $\pm$ 0.8
GluK2(R) + APV 50 $\mu\text{M}$	1057 $\pm$ 87 (22)	264 $\pm$ 19	965 $\pm$ 99 (26)	279 $\pm$ 24
	31 $\pm$ 3.2	8.5 $\pm$ 0.8	23.6 $\pm$ 2.7	7.2 $\pm$ 0.5
GluK2(R) + nifedipine 10 $\mu\text{M}$	1001 $\pm$ 114 (17)	211 $\pm$ 26	1039 $\pm$ 76 (23)	234 $\pm$ 19
	29.8 $\pm$ 3.8	7.7 $\pm$ 0.6	30.8 $\pm$ 2.8	8 $\pm$ 0.5
B. “Wild-type” cells treated with APV and nifedipine				
Control + DMSO	1091 $\pm$ 78 (10)	255 $\pm$ 20.5		
	33.8 $\pm$ 3.3	6.1 $\pm$ 0.6		
Control + APV 50 $\mu\text{M}$	1081 $\pm$ 130 (10)	270 $\pm$ 38		
	33.1 $\pm$ 5.8	6.4 $\pm$ 1.1		
Control + nifedipine 10 $\mu\text{M}$	1002 $\pm$ 172 (10)	260 $\pm$ 32		
	21.2 $\pm$ 3.5	7 $\pm$ 1.2		
C. Interneurons treated with APV and nifedipine				
Condition	MDL ( <i>n</i> )	MDS ( <i>n</i> )	PD	
Control + DMSO	329 $\pm$ 20 (21)	8.2 $\pm$ 0.7	4.3 $\pm$ 0.2	
GluK2(R) + DMSO	497 $\pm$ 53 (11), <i>P</i> = 0.005	9.5 $\pm$ 1.4	4.3 $\pm$ 0.4	
GluK2(R) + APV 50 $\mu\text{M}$	382 $\pm$ 34 (24)	10.6 $\pm$ 0.7	4.4 $\pm$ 0.3	
GluK2(R) + nifedipine 10 $\mu\text{M}$	322 $\pm$ 28 (25)	8.1 $\pm$ 0.7	4.3 $\pm$ 0.2	

## KARs for Neurite Growth

KARs have been shown to modulate differentiation of dorsal root ganglion cells (DRGs) in a biphasic manner depending on collapsin response mediator protein-2 [24]. It is postulated that early in development, during periods of structural plasticity, homo- and/or heteromeric low-affinity KARs keep neurites motile, despite their low channel conductance, low sensitivity to glutamate, fast onset of desensitization, and also slow recovery from desensitization [62, 63]. KAR activation by low agonist concentrations, e.g., by ambient glutamate, has been suggested to promote neurite outgrowth via a metabotropic signal cascade triggered by low-affinity subunits independent of their ionotropic function [20]. Later in development, high-affinity subunits increase in expression, forming heteromeric receptors which are targeted to active pre- and postsynaptic

sites [64]. Their strong ionotropic function with high channel conductance and lower desensitization rates [62, 65] arrests further neurite outgrowth [25, 66, 67], presumably by an increased uncoupling of KARs from their metabotropic actions [24].

## GluK2 Overexpression and Kainate Promote Dendritic Growth

GluK2 is enriched in pyramidal cells [68, 69]. It is particularly important for regulating cellular excitability. Evidence suggests that a metabotropic mechanism via a G protein and protein kinase C underlies this effect, which is independent of its ionotropic function, of GluK1, and of AMPARs [20]. Accordingly, GluK2 is important for network activity, e.g., in cortex and hippocampus, and for kainate-induced gamma

**Table 5** Quantitative morphometric analysis of pharmacologically treated neurons (A). Mean  $\pm$  s.e.m. of apical and basal dendritic length and segment number of pyramidal cells from layer II/III overexpressing GluK2(R) in the absence or presence of GYKI 47261. For “control + DMSO,” “GluK2(R) + DMSO,” “control + GYKI,” and “GluK2(R) + GYKI,” ANOVA on ranks vs “control + DMSO” with Dunn’s correction for multiple testing was performed followed by Mann-Whitney *U* tests. *P* values are given. ADL, apical dendritic length ( $\mu$ m); BDL, mean basal dendritic length ( $\mu$ m). The number of reconstructed cells per group given in (*n*)

Condition	Pyramidal cells in layers II/III	
	ADL ( <i>n</i> ) Segments	BDL Segments
Control + DMSO	987 $\pm$ 93 (22) 22.5 $\pm$ 2.4	250 $\pm$ 17 6.6 $\pm$ 0.4
GluK2(R) + DMSO	1537 $\pm$ 154 (20), <i>P</i> = 0.007 37.5 $\pm$ 3.9, <i>P</i> < 0.001	284 $\pm$ 20 8.4 $\pm$ 0.5
Control + GYKI 1 $\mu$ M	1003 $\pm$ 78 (22) 24 $\pm$ 2	215 $\pm$ 17 6 $\pm$ 0.4
GluK2(R) + GYKI 1 $\mu$ M	1443 $\pm$ 136 (19), <i>P</i> = 0.017 39 $\pm$ 4.3, <i>P</i> = 0.008	309 $\pm$ 33 9 $\pm$ 0.9

oscillations, the latter being stronger in supragranular cortical layers [43, 49]. In GluK2-deficient mice, kainate fails to evoke network oscillations or epileptic seizures, and even postsynaptic KAR currents were absent [50, 53]. In cortical pyramidal cells, KARs are distributed to the apical dendrites and increase in density towards distal compartments, where they locate at extrasynaptic sites [70]. There, glutamate could activate KARs along with AMPARs, e.g., with GluA3(Q)-flip, one of the growth-promoting AMPAR subunits [9] which is highly expressed in apical dendrites [71]. We suggest that the network activity elicited by 500 nM kainate triggers apical

dendritic growth in supragranular pyramidal cells via these endogenously expressed receptors. In line with our earlier study [9], blockers of NMDARs and VGCCs also abolished the GluK2-induced growth, but GluK2 still could promote its effects on growth under GYKI 47261. This suggests that, similar to AMPARs, GluK2 contributes to dendritic maturation upstream of NMDARs and VGCCs.

Our recordings revealed enhanced activity of GluK2-overexpressing neurons as well as their wild-type neighbors. Presumably, the GluK2-overexpressing pyramidal cells acted as pacemakers for the network. With GluK2 overexpression, pyramidal cell apical dendrites may grow via the action of these extra receptors or via the increased network activity that they themselves had elicited. It was a phenocopy of chronic kainate treatment. GluK2 channels contribute only marginally to postsynaptic currents [65, 72, 73], and the calcium event amplitudes of the transfectants and wild-type neighbors were not different from those in control cells. This could argue against a direct action of the overexpressed GluK2. Further, the above-mentioned wild-type neighbors did also respond with dendritic growth in a similar fashion when GluK2 transfectants were present in the same OTC, indicating that GluK2 exerts its growth-promoting effects mostly by driving network activity. On the other hand, apical dendrites remained slightly shorter and significantly less branched in pyramidal cells expressing the kinase-dead variant of TTBK2. These neurons also displayed less calcium events and were less sensitive to kainate in a dendritic injury assay, suggesting that at least a partial knockdown had been achieved with this brain-derived enzymatic tool. TTBK2-KD has been shown to reduce GluK2 surface expression in a Rab5-dependent manner [54], and a reduced amount of surface GluK2 might be responsible for the decreased excitability and the resulting slightly impaired morphology of transfected neurons. It is

**Table 6** Quantitative morphometric analysis of cells overexpressing TTBK2-KD (A). Mean  $\pm$  s.e.m. of apical and basal dendritic length and segment number of pyramidal cells from layer II/III and layer V/VI overexpressing the kinase-dead mutant of tau-tubulin kinase 2 (TTBK2-KD). ADL, apical dendritic length ( $\mu$ m); BDL, mean basal dendritic

length ( $\mu$ m). (B) Mean  $\pm$  s.e.m. of dendritic length and segment numbers of interneurons overexpressing TTBK2-KD. MDL, mean dendritic length ( $\mu$ m); MDS, mean dendritic segments; PD, number of primary dendrites. The number of reconstructed cells per group given in (*n*)

#### A. Pyramidal cells overexpressing TTBK2-KD

Condition	Pyramidal cells in layers II/III		Pyramidal cells in layers V/VI	
	ADL ( <i>n</i> ) Segments	BDL Segments	ADL ( <i>n</i> ) Segments	BDL Segments
Control	1014 $\pm$ 48 (62) 27.2 $\pm$ 1.4	246 $\pm$ 17 7.2 $\pm$ 0.4	888 $\pm$ 51 (46) 20.3 $\pm$ 1.1	291 $\pm$ 19 7.2 $\pm$ 0.5
TTBK2-KD	916 $\pm$ 42 (76) 23 $\pm$ 1.1, <i>P</i> = 0.018	259 $\pm$ 11 6.9 $\pm$ 0.3	785 $\pm$ 44 (51) 17 $\pm$ 1, <i>P</i> = 0.033	265 $\pm$ 13 6.7 $\pm$ 0.3

#### B. Interneurons overexpressing TTBK2-KD

Condition	MDL ( <i>n</i> )	MDS ( <i>n</i> )	PD
Control	317 $\pm$ 26 (18)	7 $\pm$ 0.5	4.8 $\pm$ 0.3
TTBK2-KD	388 $\pm$ 30 (25)	7.3 $\pm$ 0.6	4.3 $\pm$ 0.3

**Table 7** Quantitative morphometric analysis of cells overexpressing NETOs (A). Mean  $\pm$  s.e.m. of apical and basal dendritic length and segment number of pyramidal cells from layer II/III and layer V/VI overexpressing the indicated NETO subunits. ADL, apical dendritic length ( $\mu\text{m}$ ); BDL, mean basal dendritic length ( $\mu\text{m}$ ). (B) Mean  $\pm$  s.e.m. of dendritic length and segment numbers of interneurons

overexpressing the indicated NETO subunits. (C) Mean  $\pm$  s.e.m. of dendritic length and segment numbers of interneurons overexpressing NETO1 in the presence of the GluK1 antagonist UBP 310. MDL, mean dendritic length ( $\mu\text{m}$ ); MDS, mean dendritic segments; PD, number of primary dendrites. The number of reconstructed cells per group given in (*n*)

A. Pyramidal cells overexpressing NETOs				
Condition	Pyramidal cells in layers II/III		Pyramidal cells in layers V/VI	
	ADL ( <i>n</i> )	BDL	ADL ( <i>n</i> )	BDL
	Segments	Segments	Segments	Segments
Control	1162 $\pm$ 52 (75)	251 $\pm$ 16	1060 $\pm$ 58 (65)	256 $\pm$ 14
	27.5 $\pm$ 1.6	6.6 $\pm$ 0.5	23 $\pm$ 1.4	6.5 $\pm$ 0.4
NETO1	1373 $\pm$ 121 (28)	317 $\pm$ 27	1004 $\pm$ 88 (32)	301 $\pm$ 27
	27.6 $\pm$ 2.1	7.2 $\pm$ 0.7	18 $\pm$ 1.4	5.5 $\pm$ 0.4
NETO2	1360 $\pm$ 77 (27)	210 $\pm$ 22	1065 $\pm$ 68 (28)	218 $\pm$ 20
	43.7 $\pm$ 3.4	8.1 $\pm$ 0.7	28.6 $\pm$ 2.8	6.5 $\pm$ 0.6
B. Interneurons overexpressing NETOs				
Condition	MDL ( <i>n</i> )		MDS	PD
Control	395 $\pm$ 25 (48)		6.3 $\pm$ 0.3	4.8 $\pm$ 0.3
NETO1	501 $\pm$ 43 (39), <i>P</i> = 0.02		7 $\pm$ 0.5	4.1 $\pm$ 0.2
NETO2	333 $\pm$ 24 (22)		6.8 $\pm$ 0.7	5.3 $\pm$ 0.3
C. Interneurons overexpressing NETO1 treated with UBP 310				
Control DMSO	403 $\pm$ 29 (17)		6.9 $\pm$ 0.6	4.5 $\pm$ 0.2
NETO1 + UBP 310 1 $\mu\text{M}$	380 $\pm$ 28 (18)		6.8 $\pm$ 0.6	5.4 $\pm$ 0.4

unlikely that other receptors, e.g., AMPARs, became internalized, because that would have likely resulted in a reduction of calcium event amplitudes. This has been seen in neurons after shRNA knockdown of the AMPAR-trafficking TARP  $\gamma$ -8, and dendritic growth is impaired in these neurons [10]. Although the data of the TTBK2-KD experiments is interesting since it had directly opposite effects to GluK2 overexpression, it should still be considered with caution. At present, we cannot exclude that TTBK2-KD could have had unknown effects on various other receptors (KARs or non-KARs) or intracellular pathways which might contribute to the outcomes we discovered. Still, if for example GluK1 would have been affected by TTBK2-KD in a similar manner than GluK2, the interneurons should have been affected in a similar way. However, this was not the case. GluK4 or GluK5 could only be affected if coexpressed in heterotetramers with either GluK1 or GluK2.

Basal dendrites are known to employ different mechanisms for growth [74] and display a more protracted, activity-independent development [75]. This could explain why neither kainate treatment nor manipulation of AMPARs could promote basal dendrite maturation.

Interestingly, interneurons overexpressing GluK2 responded also with dendritic growth. They were in a more active network wired up with pyramidal cells overexpressing GluK2. It could be possible that the growth of GluK2 overexpressing interneurons was solely mediated by the increased

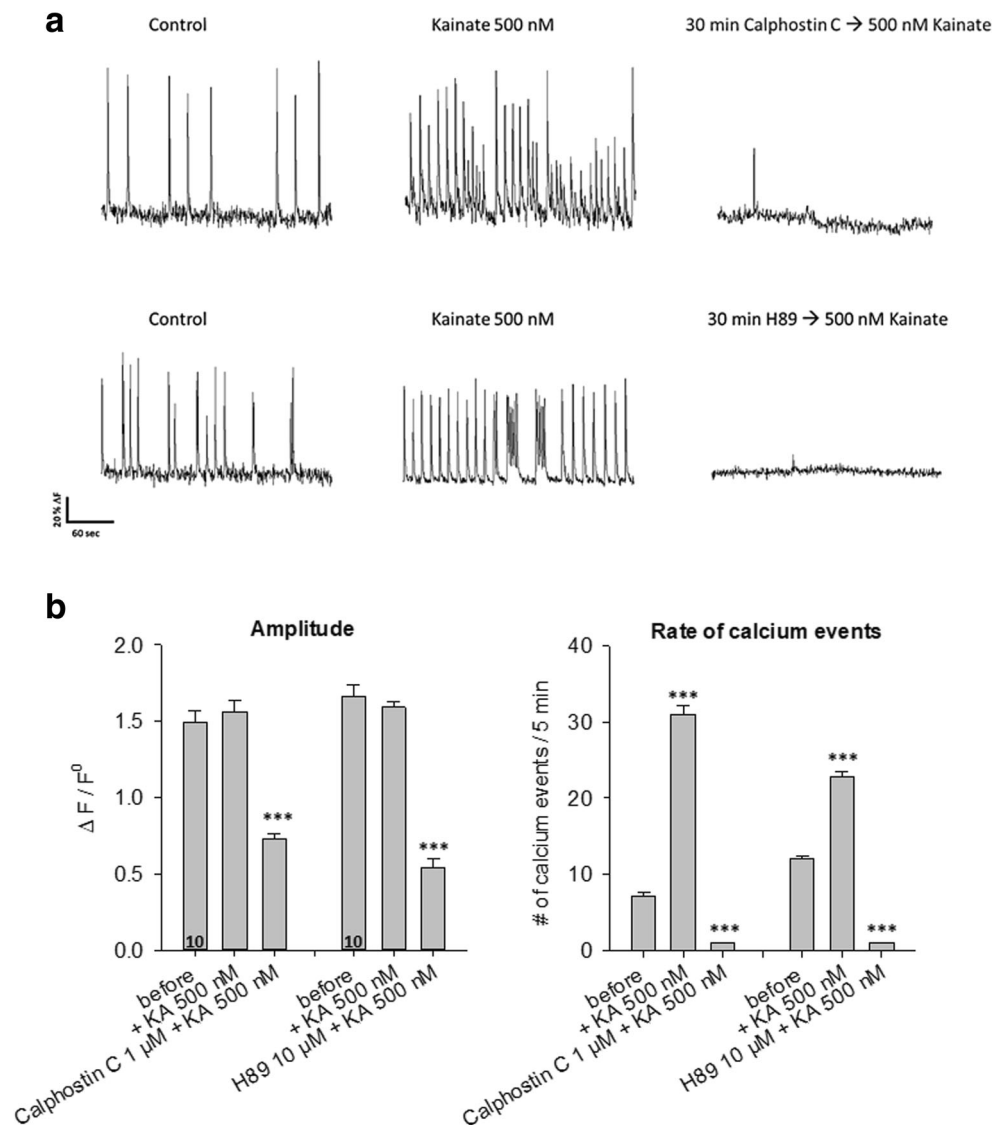
network activity without any direct effects of GluK2. However, a kainate-induced increase of network activity (Table 1B) was not sufficient to promote dendritic growth of interneurons. Therefore, the increased maturation of GluK2-transfected interneurons could possibly reflect the combined effect of increased network activity and augmented individual excitability (evoked by GluK2 overexpression).

Our experiments with the inhibitors calphostin C (blocks PKC) and H89 (blocks PKA) indicate that the metabotropic actions of KARs on transmitter release and cellular excitability are involved in KAR-mediated pacing of the network, and possibly also the growth-promoting actions. The KAR action on postsynaptic excitability is predominantly PKC-dependent [20] while the presynaptic action is mainly PKA-dependent [20, 22]. Based on our observations, both of the described KAR-mediated metabotropic pathways are required for the observed effects of KARs on driving developing networks and dendritic maturation in the early postnatal time window.

### GluK1 Increase Dendritic Complexity Only in Interneurons

Interneurons strongly express KARs containing the GluK1 subunit, and a majority also expresses GluK2 [17, 53, 56, 57]. GluK1 has a small conductance and has been reported to open, close, and desensitize faster than GluK2 by at least 2-fold [76]. The predominant KAR is likely a GluK1/2

**Fig. 7** Kainate fails to increase network activity in the presence of PKC or PKA inhibitors. Two large batches of cultures were divided into two groups: one for calphostin C and one for H89. From the two batches,  $2 \times 5$  OTC have been recorded (a). Representative traces of spontaneous calcium events in wild-type neurons at DIV 8 loaded with OGB-1 AM (expressed as  $\Delta F/F^0$ ). Activity was first recorded in the absence or presence of 500 nM kainate. Subsequently, the PKC inhibitor calphostin C (1  $\mu$ M) or the PKA inhibitor H89 (10  $\mu$ M) were incubated for 30 min in the recording chamber. Afterwards, the inhibitors were washed out with ACSF containing 500 nM kainate for 10 min, activity was recorded for 5 min under 500 nM kainate (trace shown above). In both conditions, kainate failed to elicit network activity. **b** Quantitative analysis (mean  $\pm$  s.e.m.) of amplitudes and frequencies of spontaneous calcium events before and after the treatment with calphostin C or H89, respectively. Both inhibitors almost completely abolished network activity and prevented the effects of 500 nM kainate recorded prior to inhibitor incubation. Numbers of analyzed OTCs are given within bars. \*\*\*,  $P < 0.001$  for treatment versus control group



heteromer, which displays 30% faster desensitization and a 40% slower recovery from desensitization than homomeric GluK2 [69]. Thus, in wild-type interneurons treated with 500 nM kainate, the contribution of the KARs to postsynaptic currents might be too small to trigger growth to any detectable extent. In contrast, overexpression of GluK2 could lead to more homomeric receptors, and overexpression did elicit dendritic elongation.

Overexpression of GluK1 elicited a growth response selective of interneurons, elongation and branching were enhanced. Further, the ATPA-evoked depression of network activity and the ATPA-evoked dendritic growth selectively of interneurons, along with the impaired growth under UBP 310, indicate a role of endogenous GluK1. These observations may be the direct consequence of GluK1 activation in interneurons. Indeed, ATPA depolarizes interneurons [48], and this can prevent seizure propagation [47], whereas a GluK1 deficit leads to higher susceptibility to kainate-induced seizures [50]. GluK1-

containing KARs can downregulate synaptic transmission [77, 78], and GluK1-containing KARs on interneurons regulate inhibition by enhancing GABA release [79]. However, although KARs can be involved in postsynaptic transmission in the cortex [72], their currents are rather small [73, 80]. Intriguingly, support for a direct effect scenario comes from our finding that NETO1 exclusively promotes dendritic maturation of interneurons, an effect that was abolished by treatment with UBP 310. A recent study shows that NETO1, by increasing the trafficking of GluK1, is required for KAR-mediated somatodendritic excitation of cholecystinin-, parvalbumin-, and somatostatin-containing interneurons [61]. Both NETOs were ineffective in pyramidal cells. Here, selected type-I TARPs exclusively promote growth [10]. This could indicate that the two major cortical neuron classes employ different iGluR auxiliary proteins to regulate dendritic maturation.

Alternatively, an indirect effect might be possible. GluK1 is expressed in presynaptic glutamatergic terminals and

increases glutamate release [26, 81, 82]. Thus, overexpression of GluK1 in pyramidal cell presynapses as well as activation by ATPA of GluK1 in wild-type presynapses may enhance the glutamatergic input to interneurons, which then respond with dendritic growth. However, in this scenario, the glutamate release onto pyramidal cells should also increase, and a subsequent activation of AMPARs/NMDARs should then elicit dendritic growth. However, this was not the case, and this would argue for the direct effect scenario.

In summary, the present study provides insight on how certain KAR subunits and their auxiliary partners, the NETOs, contribute to the morphological and physiological maturation of rat visual cortical neurons during the early postnatal period.

**Acknowledgements** We thank Andrea Räk, Sabine Schönfelder, and Christian Riedel for technical support. We thank Prof. Nathalie Strutz-Seebohm, University Münster, for providing the TTBK2-KD plasmid. We thank Prof. Andreas Reiner, Ruhr University Bochum, for discussion. We thank Bente Janssen-Weets and Felix Burgmann for help with reconstructions during their BSc thesis work.

**Author Contribution** AJ, MIKH, and PW designed experiments. AJ, MIKH, SG, SP, and PW performed experiments. AJ and PW did the data management and interpretation. AJ and PW wrote the manuscript. MH commented on the manuscript. All authors approved the final version.

**Funding Information** Supported by Deutsche Forschungsgemeinschaft grants WA 541/9-1 and 541/9-2.

## Compliance with Ethical Standards

**Conflict of Interest** The authors declare that they do not have any conflict of interest.

## References

- Hollmann M, Heinemann S (1994) Cloned glutamate receptors. *Annu Rev Neurosci* 17:31–108. <https://doi.org/10.1146/annurev.ne.17.030194.000335>
- Lodge D (2009) The history of the pharmacology and cloning of ionotropic glutamate receptors and the development of idiosyncratic nomenclature. *Neuropharmacology* 56:6–21. <https://doi.org/10.1016/j.neuropharm.2008.08.006>
- Wu GY, Cline HT (1998) Stabilization of dendritic arbor structure in vivo by CaMKII. *Science* 279:222–226. <https://doi.org/10.1126/science.279.5348.222>
- Rajan I, Cline HT (1998) Glutamate receptor activity is required for normal development of tectal cell dendrites in vivo. *J Neurosci* 18:7836–7846. <https://doi.org/10.1523/JNEUROSCI.18-19-07836.1998>
- Sin WC, Haas K, Ruthazer ES, Cline HT (2002) Dendrite growth increased by visual activity requires NMDA receptor and Rho GTPases. *Nature* 419:475–480. <https://doi.org/10.1038/nature00987>
- Iwasato T, Datwani A, Wolf AM, Nishiyama H, Taguchi Y, Tonegawa S, Knöpfel T, Erzurumlu RS et al (2000) Cortex-restricted disruption of NMDAR1 impairs neuronal patterns in the barrel cortex. *Nature* 406:726–731. <https://doi.org/10.1038/35021059>
- Lee L-J, Lo F-S, Erzurumlu RS (2005) NMDA receptor-dependent regulation of axonal and dendritic branching. *J Neurosci* 25:2304–2311. <https://doi.org/10.1523/JNEUROSCI.4902-04.2005>
- Haas K, Li J, Cline HT (2006) AMPA receptors regulate experience-dependent dendritic arbor growth in vivo. *Proc Natl Acad Sci U S A* 103:12127–12131. <https://doi.org/10.1073/pnas.0602670103>
- Hamad MIK, Ma-Högemeier Z-L, Riedel C, Conrads C, Veitinger T, Habijan T, Schulz J-N, Krause M et al (2011) Cell class-specific regulation of neocortical dendrite and spine growth by AMPA receptor splice and editing variants. *Development* 138:4301–4313. <https://doi.org/10.1242/dev.071076>
- Hamad MIK, Jack A, Klatt O, Lorkowski M, Strasdeit T, Kott S, Sager C, Hollmann M et al (2014) Type I TARPs promote dendritic growth of early postnatal neocortical pyramidal cells in organotypic cultures. *Development* 141:1737–1748. <https://doi.org/10.1242/dev.099697>
- Traynelis SF, Wollmuth LP, McBain CJ, Menniti FS, Vance KM, Ogden KK, Hansen KB, Yuan H et al (2010) Glutamate receptor ion channels. *Pharmacol Rev* 62:405–496. <https://doi.org/10.1124/pr.109.002451>
- Herb A, Burnashev N, Werner P, Sakmann B, Wisden W, Seeburg PH (1992) The KA-2 subunit of excitatory amino acid receptors shows widespread expression in brain and forms ion channels with distantly related subunits. *Neuron* 8:775–785. [https://doi.org/10.1016/0896-6273\(92\)90098-X](https://doi.org/10.1016/0896-6273(92)90098-X)
- Contractor A, Mülle C, Swanson GT (2011) Kainate receptors coming of age. *Trends Neurosci* 34:154–163. <https://doi.org/10.1016/j.tins.2010.12.002>
- Hadzic M, Jack A, Wahle P (2017) Ionotropic glutamate receptors. *J Comp Neurol* 525:976–1033. <https://doi.org/10.1002/cne.24103>
- Wisden W, Seeburg PH (1993) A complex mosaic of high-affinity kainate receptors in rat brain. *J Neurosci* 13:3582–3598. <https://doi.org/10.1523/JNEUROSCI.13-08-03582.1993>
- Bernard A, Ferhat L, Dessi F, Charton G, Represa A, Ben-Ari Y, Khrestchatsky M (1999) Q/R editing of the rat GluR5 and GluR6 kainate receptors in vivo and in vitro. *Eur J Neurosci* 11:604–616. <https://doi.org/10.1046/j.1460-9568.1999.00479.x>
- Bahn S, Volk B, Wisden W (1994) Kainate receptor gene expression in the developing rat brain. *J Neurosci* 14:5525–5547. <https://doi.org/10.1523/JNEUROSCI.14-09-05525.1994>
- Paschen W, Dux E, Djuricic B (1994) Developmental changes in the extent of RNA editing of glutamate receptor subunit GluR5 in rat brain. *Neurosci Lett* 174:109–112. [https://doi.org/10.1016/0304-3940\(94\)90131-7](https://doi.org/10.1016/0304-3940(94)90131-7)
- Paschen W, Schmitt J, Gissel C, Dux E (1997) Developmental changes of RNA editing of glutamate receptor subunits GluR5 and GluR6. *Brain Res* 98:271–280. [https://doi.org/10.1016/S0165-3806\(96\)00193-9](https://doi.org/10.1016/S0165-3806(96)00193-9)
- Valbuena S, Lerma J (2016) Non-canonical signaling, the hidden life of ligand-gated ion channels. *Neuron* 92:316–329. <https://doi.org/10.1016/j.neuron.2016.10.016>
- Sihra TS, Rodríguez-Moreno A (2013) Presynaptic kainate receptor mediated bidirectional modulatory actions: mechanisms. *Neurochem Int* 62:982–987. <https://doi.org/10.1016/j.neuint.2013.03.012>
- Negrete-Díaz JV, Sihra TS, Flores G, Rodríguez-Moreno A (2018) Non-canonical mechanisms of presynaptic kainate receptors controlling glutamate release. *Front Mol Neurosci* 11:128. <https://doi.org/10.3389/fnmol.2018.00128>
- Monnerie H, Le Roux PD (2006) Glutamate receptor agonist kainate enhances primary dendrite number and length from immature mouse cortical neurons in vitro. *J Neurosci Res* 83:944–956. <https://doi.org/10.1002/jnr.20805>

24. Marques JM, Rodrigues RJ, Valbuena S, Rozas JL, Selak S, Marin P, Aller MI, Lerma J (2013) CRMP2 tethers kainate receptor activity to cytoskeleton dynamics during neuronal maturation. *J Neurosci* 33:18298–18310. <https://doi.org/10.1523/JNEUROSCI.3136-13.2013>
25. Joseph DJ, Williams DJ, MacDermott AB (2011) Modulation of neurite outgrowth by activation of calcium-permeable kainate receptors expressed by rat nociceptive-like dorsal root ganglion neurons. *Dev Neurobiol* 71:818–835. <https://doi.org/10.1002/dneu.20906>
26. Campbell SL, Mathew SS, Hablitz JJ (2007) Pre- and postsynaptic effects of kainate on layer II/III pyramidal cells in rat neocortex. *Neuropharmacology* 53:37–47. <https://doi.org/10.1016/j.neuropharm.2007.04.008>
27. Nasu-Nishimura Y, Jaffe H, Isaac JTR, Roche KW (2010) Differential regulation of kainate receptor trafficking by phosphorylation of distinct sites on GluR6. *J Biol Chem* 285:2847–2856. <https://doi.org/10.1074/jbc.M109.081141>
28. Park Y, Jo J, Isaac JTR, Cho K (2006) Long-term depression of kainate receptor-mediated synaptic transmission. *Neuron* 49:95–106. <https://doi.org/10.1016/j.neuron.2005.11.035>
29. Petrovic MM, Viana da Silva S, Clement JP, Vyklicky L, Mulle C, González-González IM, Henley JM (2017) Metabotropic action of postsynaptic kainate receptors triggers hippocampal long-term potentiation. *Nat Neurosci* 20:529–539. <https://doi.org/10.1038/nn.4505>
30. Juuri J, Clarke VRJ, Lauri SE, Taira T (2010) Kainate receptor-induced ectopic spiking of CA3 pyramidal neurons initiates network bursts in neonatal hippocampus. *J Neurophysiol* 104:1696–1706. <https://doi.org/10.1152/jn.00840.2009>
31. Orav, E., Atanasova, T., Shintyapina, A., Kesaf, S., Kokko, M., Partanen, J., Taira, T., Lauri, S.E. (2017). NETO1 guides development of glutamatergic connectivity in the hippocampus by regulating axonal kainate receptors. *eNeuro* 4. <https://doi.org/10.1523/ENEURO.0048-17.2017>
32. Vernon CG, Swanson GT (2017) Neto2 assembles with kainate receptors in DRG neurons during development and modulates neurite outgrowth in adult sensory neurons. *J Neurosci* 37:3352–3363. <https://doi.org/10.1523/JNEUROSCI.2978-16.2017>
33. Wirth MJ, Wahle P (2003) Biolistic transfection of organotypic cultures of rat visual cortex using a handheld device. *J Neurosci Methods* 125:45–54. [https://doi.org/10.1016/S0165-0270\(03\)00024-4](https://doi.org/10.1016/S0165-0270(03)00024-4)
34. Bouskila M, Esoof N, Gay L, Fang EH, Deak M, Begley MJ, Cantley LC, Prescott A et al (2011) TTBK2 kinase substrate specificity and the impact of spinocerebellar-ataxia-causing mutations on expression, activity, localization and development. *Biochem J* 437:157–167. <https://doi.org/10.1042/BJ20110276>
35. Chen TW, Wardill TJ, Sun Y, Pulver SR, Renninger SL, Baohan A, Schreiter ER, Kerr RA et al (2013) Ultrasensitive fluorescent proteins for imaging neuronal activity. *Nature* 499(7458):295–300. <https://doi.org/10.1038/nature12354>
36. Yang B, Treweek JB, Kulkarni RP, Deverman BE, Chen CK, Lubeck E, Shah S, Cai L et al (2014) 808 Single-cell phenotyping within transparent intact tissue through whole-body clearing. *Cell* 158(4):945–958. <https://doi.org/10.1016/j.cell.2014.07.017>
37. Hamad MIK, Krause M, Wahle P (2015) Improving AM ester calcium dye loading efficiency. *J Neurosci Methods* 240:48–60. <https://doi.org/10.1016/j.jneumeth.2014.11.010>
38. Pologruto TA, Sabatini BL, Svoboda K (2003) ScanImage. *Biomed Eng Online* 2:13. <https://doi.org/10.1186/1475-925X-2-13>
39. Rasband WS (1997–2012) ImageJ. National Institutes of Health, Bethesda, MD, USA. Available online at: <https://imagej.nih.gov/ij/>
40. Hoerder-Suabedissen A, Paulsen O, Molnar Z (2008) Thalamocortical maturation in mice is influenced by body weight. *J Comp Neurol* 511:415–420. <https://doi.org/10.1002/cne.21853>
41. Oh E, Maejima T, Liu C, Deneris E, Herlitze S (2010) Substitution of 5-HT1A receptor signaling by a light-activated G protein-coupled receptor. *J Biol Chem* 285:30825–30836. <https://doi.org/10.1074/jbc.M110.147298>
42. Lauri SE, Taira T (2011) Role of kainate receptors in network activity during development. *Adv Exp Med Biol* 717:81–91. [https://doi.org/10.1007/978-1-4419-9557-5\\_8](https://doi.org/10.1007/978-1-4419-9557-5_8)
43. Beed PS, Salmen B, Schmitz D (2009) GluK2-mediated excitability within the superficial layers of the entorhinal cortex. *PLoS One* 4:e5576. <https://doi.org/10.1371/journal.pone.0005576>
44. Clarke VR, Ballyk BA, Hoo KH, Mandelzys A, Pellizzari A, Bath CP, Thomas J, Sharpe EF et al (1997) A hippocampal GluR5 kainate receptor regulating inhibitory synaptic transmission. *Nature* 389:599–603. <https://doi.org/10.1038/39315>
45. Cossart R, Esclapez M, Hirsch JC, Bernard C, Ben-Ari Y (1998) GluR5 kainate receptor activation in interneurons increases tonic inhibition of pyramidal cells. *Nat Neurosci* 1:470–478. <https://doi.org/10.1038/2185>
46. Frerking M, Malenka RC, Nicoll RA (1998) Synaptic activation of kainate receptors on hippocampal interneurons. *Nat Neurosci* 1:479–486. <https://doi.org/10.1038/2194>
47. Khalilov I, Hirsch J, Cossart R, Ben-Ari Y (2002) Paradoxical anti-epileptic effects of a GluR5 agonist of kainate receptors. *J Neurophysiol* 88:523–527. <https://doi.org/10.1152/jn.2002.88.1.523>
48. Rodríguez-Moreno A, López-García JC, Lerma J (2000) Two populations of kainate receptors with separate signaling mechanisms in hippocampal interneurons. *Proc Natl Acad Sci U S A* 97:1293–1298. <https://doi.org/10.1073/pnas>
49. Cunningham MO, Davies CH, Buhl EH, Kopell N, Whittington MA (2003) Gamma oscillations induced by kainate receptor activation in the entorhinal cortex in vitro. *J Neurosci* 23:9761–9769. <https://doi.org/10.1523/JNEUROSCI.23-30-09761.2003>
50. Fisahn A, Contractor A, Traub RD, Buhl EH, Heinemann SF, McBain CJ (2004) Distinct roles for the kainate receptor subunits GluR5 and GluR6 in kainate-induced hippocampal gamma oscillations. *J Neurosci* 24:9658–9668. <https://doi.org/10.1523/JNEUROSCI.2973-04.2004>
51. Melyan Z, Wheal HV, Lancaster B (2002) Metabotropic-mediated kainate receptor regulation of IsAHP and excitability in pyramidal cells. *Neuron* 34:107–114. [https://doi.org/10.1016/S0896-6273\(02\)00624-4](https://doi.org/10.1016/S0896-6273(02)00624-4)
52. Melyan Z, Lancaster B, Wheal HV (2004) Metabotropic regulation of intrinsic excitability by synaptic activation of kainate receptors. *J Neurosci* 24:4530–4534. <https://doi.org/10.1523/JNEUROSCI.5356-03.2004>
53. Mulle C, Sailer A, Pérez-Otaño I, Dickinson-Anson H, Castillo PE, Bureau I, Maron C, Gage FH et al (1998) Altered synaptic physiology and reduced susceptibility to kainate-induced seizures in GluR6-deficient mice. *Nature* 392:601–605. <https://doi.org/10.1038/33408>
54. Nieding K, Matschke V, Meuth SG, Lang F, Seeböhm G, Strutz-Seeböhm N (2016) Tau tubulin kinase TTBK2 sensitivity of glutamate receptor GluK2. *Cell Physiol Biochem* 39:1444–1452. <https://doi.org/10.1159/000447847>
55. Fièvre S, Carta M, Chamma I, Labrousse V, Thoumine O, Mulle C (2016) Molecular determinants for the strictly compartmentalized expression of kainate receptors in CA3 pyramidal cells. *Nat Commun* 7:12738. <https://doi.org/10.1038/ncomms12738>
56. Bureau I, Bischoff S, Heinemann SF, Mulle C (1999) Kainate receptor-mediated responses in the CA1 field of wild-type and GluR6-deficient mice. *J Neurosci* 19:653–663. <https://doi.org/10.1523/JNEUROSCI.19-02-00653.1999>
57. Petralia RS, Wang YX, Wenthold RJ (1994) Histological and ultrastructural localization of the kainate receptor subunits, KA2 and GluR6/7, in the rat nervous system using selective antipeptide

- antibodies. *J Comp Neurol* 349:85–110. <https://doi.org/10.1002/cne.903490107>
58. Copits BA, Swanson GT (2012) Dancing partners at the synapse. *Nat Rev Neurosci* 13:675–686. <https://doi.org/10.1038/nrn3335>
  59. Zhang W, St-Gelais F, Grabner CP, Trinidad JC, Sumioka A, Morimoto-Tomita M, Kim KS, Straub C et al (2009) A transmembrane accessory subunit that modulates kainate-type glutamate receptors. *Neuron* 61:385–396. <https://doi.org/10.1111/ejn.12519>
  60. Palacios-Filardo J, Aller MI, Lerma J (2016) Synaptic targeting of kainate receptors. *Cereb Cortex* 26:1464–1472. <https://doi.org/10.1093/cercor/bhu244>
  61. Wyeth MS, Pelkey KA, Yuan X, Vargish G, Johnston AD, Hunt S, Fang C, Abebe D et al (2017) Neto auxiliary subunits regulate interneuron somatodendritic and presynaptic kainate receptors to control network inhibition. *Cell Rep* 20:2156–2168. <https://doi.org/10.1016/j.celrep.2017.08.017>
  62. Fisher JL, Mott DD (2011) Distinct functional roles of subunits within the heteromeric kainate receptor. *J Neurosci* 31:17113–17122. <https://doi.org/10.1523/JNEUROSCI.3685-11.2011>
  63. Paternain AV, Rodríguez-Moreno A, Villarroya A, Lerma J (1998) Activation and desensitization properties of native and recombinant kainate receptors. *Neuropharmacology* 37:1249–1259. [https://doi.org/10.1016/S0028-3908\(98\)00098-7](https://doi.org/10.1016/S0028-3908(98)00098-7)
  64. Fernandes HB, Catches JS, Petralia RS, Copits BA, Xu J, Russell TA, Swanson GT, Contractor A (2009) High-affinity kainate receptor subunits are necessary for ionotropic but not metabotropic signaling. *Neuron* 63:818–829. <https://doi.org/10.1016/j.neuron.2009.08.010>
  65. Barberis A, Sachidhanandam S, Mulle C (2008) GluR6/KA2 kainate receptors mediate slow-deactivating currents. *J Neurosci* 28:6402–6406. <https://doi.org/10.1523/JNEUROSCI.1204-08.2008>
  66. Ibarretxe G, Perais D, Jaskolski F, Vimeney A, Mulle C (2007) Fast regulation of axonal growth cone motility by electrical activity. *J Neurosci* 27:7684–7695. <https://doi.org/10.1523/JNEUROSCI.1070-07.2007>
  67. Tashiro A, Dunaevsky A, Blazeski R, Mason CA, Yuste R (2003) Bidirectional regulation of hippocampal mossy fiber filopodial motility by kainate receptors. *Neuron* 38:773–784. [https://doi.org/10.1016/S0896-6273\(03\)00299-X](https://doi.org/10.1016/S0896-6273(03)00299-X)
  68. Dai W-M, Christensen KV, Egebjerg J, Ebert B, Lambert JDC (2002) Correlation of the expression of kainate receptor subtypes to responses evoked in cultured cortical and spinal cord neurones. *Brain Res* 926:94–107. [https://doi.org/10.1016/S0006-8993\(01\)03308-X](https://doi.org/10.1016/S0006-8993(01)03308-X)
  69. Paternain AV, Herrera MT, Nieto MA, Lerma J (2000) GluR5 and GluR6 kainate receptor subunits coexist in hippocampal neurons and coassemble to form functional receptors. *J Neurosci* 20:196–205. <https://doi.org/10.1523/JNEUROSCI.20-01-00196.2000>
  70. Eder M, Becker K, Rammes G, Schierloh A, Azad SC, Zieglgänsberger W, Dodt H-U (2003) Distribution and properties of functional postsynaptic kainate receptors on neocortical layer V pyramidal neurons. *J Neurosci* 23:6660–6670. <https://doi.org/10.1523/JNEUROSCI.23-16-06660.2003>
  71. Sommer B, Keinänen K, Verdoorn TA, Wisden W, Burnashev N, Herb A, Köhler M, Takagi T et al (1990) Flip and flop: a cell-specific functional switch in glutamate-operated channels of the CNS. *Science* 249:1580–1585. <https://doi.org/10.1126/science.1699275>
  72. Ali AB (2003) Involvement of post-synaptic kainate receptors during synaptic transmission between unitary connections in rat neocortex. *Eur J Neurosci* 17:2344–2350. <https://doi.org/10.1046/j.1460-9568.2003.02677.x>
  73. Swanson GT, Feldmeyer D, Kaneda M, Cull-Candy SG (1996) Effect of RNA editing and subunit co-assembly single-channel properties of recombinant kainate receptors. *J Physiol* 492:129–142. <https://doi.org/10.1113/jphysiol.1996.sp021295>
  74. Chow DK, Groszer M, Pribadi M, Machnicki M, Carmichael ST, Liu X, Trachtenberg JT (2009) Laminar and compartmental regulation of dendritic growth in mature cortex. *Nat Neurosci* 12:116–118. <https://doi.org/10.1038/nn.2255>
  75. Romand S, Wang Y, Toledo-Rodriguez M, Markram H (2011) Morphological development of thick-tufted layer v pyramidal cells in the rat somatosensory cortex. *Front Neuroanat* 5:5. <https://doi.org/10.3389/fnana.2011.00005>
  76. Han Y, Wang C, Park JS, Niu L (2012) Channel-opening kinetic mechanism of wild-type GluK1 kainate receptors and a C-terminal mutant. *Biochemistry* 51:761–768. <https://doi.org/10.1021/bi201446z>
  77. Salmen B, Beed PS, Ozdogan T, Maier N, Johanning FW, Winterer J, Breustedt J, Schmitz D (2012) GluK1 inhibits calcium dependent and independent transmitter release at associational/commissural synapses in area CA3 of the hippocampus. *Hippocampus* 22:57–68. <https://doi.org/10.1002/hipo.20846>
  78. Vignes M, Clarke VR, Parry MJ, Bleakman D, Lodge D, Ornstein PL, Collingridge GL (1998) The GluR5 subtype of kainate receptor regulates excitatory synaptic transmission in areas CA1 and CA3 of the rat hippocampus. *Neuropharmacology* 37:1269–1277. [https://doi.org/10.1016/S0028-3908\(98\)00148-8](https://doi.org/10.1016/S0028-3908(98)00148-8)
  79. Wu L-J, Xu H, Ren M, Zhuo M (2007) Genetic and pharmacological studies of GluR5 modulation of inhibitory synaptic transmission in the anterior cingulate cortex of adult mice. *Dev Neurobiol* 67:146–157. <https://doi.org/10.1002/dneu.20331>
  80. Wu L-J, Zhao M-G, Toyoda H, Ko SW, Zhuo M (2005) Kainate receptor-mediated synaptic transmission in the adult anterior cingulate cortex. *J Neurophysiol* 94:1805–1813. <https://doi.org/10.1152/jn.00091.2005>
  81. Andrade-Talavera Y, Duque-Feria P, Negrete-Díaz JV, Sihra TS, Flores G, Rodríguez-Moreno A (2012) Presynaptic kainate receptor-mediated facilitation of glutamate release involves Ca<sup>2+</sup>-calmodulin at mossy fiber-CA3 synapses. *J Neurochem* 122:891–899. <https://doi.org/10.1111/j.1471-4159.2012.07844.x>
  82. Rodríguez-Moreno A, Sihra TS (2013) Presynaptic kainate receptor-mediated facilitation of glutamate release involves Ca<sup>2+</sup>-calmodulin and PKA in cerebrocortical synaptosomes. *FEBS Lett* 587:788–792. <https://doi.org/10.1016/j.febslet.2013.01.071>